AN INVESTIGATION OF THE EFFECT OF DIFFERENT ADDITIVES ON THE COMPRESSIVE AND FLEXURAL STRENGTH OF RAMMED EARTH

by

Aiham Alskif

A Thesis Submitted in

Partial Fulfillment of the

Requirements for the Degree of

Master of Science

in Engineering

at

The University of Wisconsin-Milwaukee

December 2016

ABSTRACT

AN INVESTIGATION OF THE EFFECT OF DIFFERENT ADDITIVES ON THE COMPRESSIVE AND FLEXURAL STRENGTH OF RAMMED EARTH

by

Aiham Alskif

The University of Wisconsin-Milwaukee, 2016
Under the Supervision of Professor Adeeb Rahman

The main objective of this research is to study the effect of using different additives on the compressive and flexural strength of rammed earth structures. Different ratios of fly ash, and/or cement were added to the soil to identify their influence on the compressive strength. Recycled fiber materials were used to wrap and reinforce the cement-soil specimens in order to enhance the flexural strength of beams and control the cracks and the mode of failure. The study finds that adding cement to soil has significant effect on the soil strength, and it causes a remarkable increase in the strength while adding fly ash does not increase the compressive strength and it results in elastic modulus reduction. Furthermore, it is concluded that wrapping and reinforcing the specimens by burlap cloth or fiber mesh do not improve the flexural strength due to the weak bond with the cement-soil material. However, when a beam is reinforced by glass fiber exhibited improvement in the flexural strength and it experienced a plastic behavior after the proportional limit and it was able to absorb a large amount of energy without failure.

TABLE OF CONTENTS

LIST OF FIGURES

LIST OF TABLES

ACKNOWLEDGEMENTS

I would like to express my appreciation to all those who gave me the possibility to complete this Dissertation. I would like to express my deepest gratitude to my advisor Professor Adeeb Rahman for his guidance and caring throughout my degree. My gratitude also to my committee members Professor Ben Church and Professor Rani El hajjar for their support. Professor Ben Church who gave me his invaluable time and guided me to use the material furnace, and professor Rani El-hajjar who provided me with extremely useful information for my thesis. I also would like to give my special thanks to the members of the department of civil engineering in the University of Wisconsin Milwaukee, especially Mr Rahim Rashidi who provided me with his knowledge and access to the concrete and the mechanics of material labs, and PhD student Saaeed Yazadani Kachooie for his knowledge and giving me access to the geotechnical lab.

Finally, I wish to express my love to my family for their endless love and support.

Thank you very much

1. Introduction

Figure 1: The ruins of a Han dynasty (202 BCE – 220 CE) Chinese watchtower made of rammed earth at Dunhuang (*Source* weikipedia)

Rammed earth is a method used in the construction of buildings which has been around since the ancient ages. This method used natural materials such as gravel, sand and clay which were compacted with a small portion of water. Recently, much attention has been given to this method as there is a growing interest in using natural materials with low carbon and more sustainability. In fact, using local soil will result in reduction of costs and decrease of greenhouse gas emissions. In addition, it has a good performance in heat resistance, sound insulation, durability, and structural capability. Therefore, Rammed earth construction has been used mainly in building bearing walls and foundations. Hence, its compressive strength is the most important property engineers have examined. Furthermore, Cement percentage, typically between 5% and 12%, was added to the natural soil to improve the strength and durability before the mix was poured into a form and compacted at the optimum moisture content of the soil.

Figure 2 photo of Phoenix Zoo entrance that was made of rammed earth [Source: wdm Architects]

2. Literature Review

Researchers have studied the characteristics of rammed earth and the properties of appropriate soil used in this system. They have reported the influence of adding cement to soil in terms of compressive strength. Also, they examined how the density of compacted soil contributes to increased strength. Reddy and Kumar (2010) conducted experiments and reported the effect of particular factors on the compaction characteristics and physical properties of cement stabilized soil. Some of these factors are the influence of various cement and soil content, moulding water content on the compressive strength of cement stabilized soils, and the effect of delayed compaction on compaction characteristics and strength. Reddy and Kumar indicated that compressive strength is increased by increasing the cement content, dry density, or moulding moisture contents. They compiled that compacting soil of 1800 kg/m^3 density with cement content between 5 and 12% raises the strength about 300% from 1.5MPa to 5 MPa. As shown in figure 3.

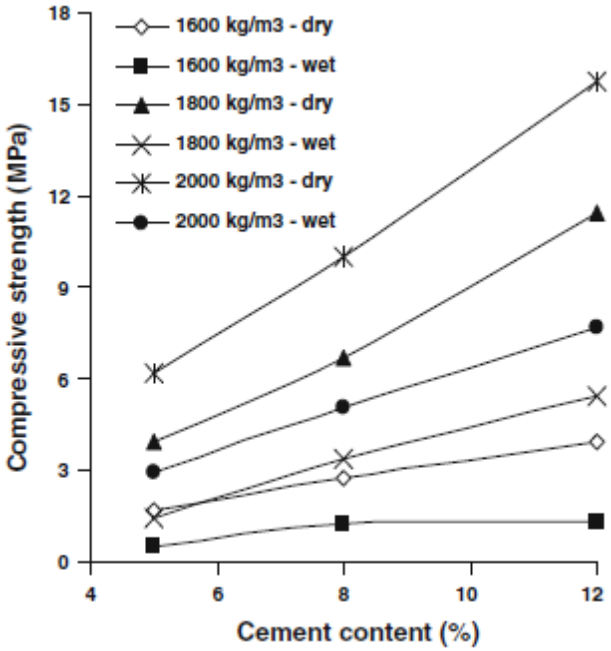

Figure 3: Cement content versus compressive strength by Reddy and Kumar (2010)

On the other hand, their study showed that strength decreases due to the delay of compaction as it is hard to obtain higher density. After adding water to the rammed earth mix, cement fluid will start to set and harden over the time creating bonds between the mix particles. Consequently, compaction after cement set would result in breaking the bond between the mix component, thus strength fell down. Furthermore, they concluded that the cement content does not affect the optimum moisture content nor the maximum dry density of the mix, and the optimum moisture content increases as the clay content of soil increases. Moreover, Reddy and Kumar (2010) studied the correlation between stress and the strain in addition to the elastic properties for the cement stabilized rammed earth (CSRE). They found that CSRE experienced elastic behavior, as the relationship between the stress and strain is linear before stress hits the maximum value, followed by significant deformation for the most samples. Finally, samples experienced sudden shear failure and diagonal cracks grew across the thickness of the sample.

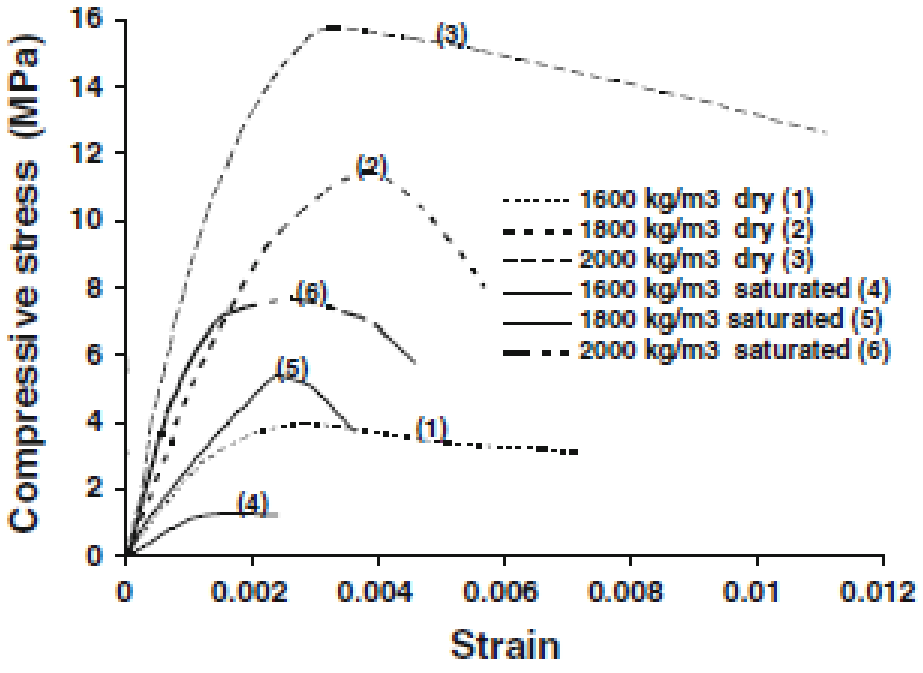

Figure 4: Stress-strain relationships for CSRE compacted with 12% cement by Reddy and Kumar (2010)

Studying the characteristic properties of cement stabilized rammed earth using a stress-strain curve, Tripura and Singh (2014) showed that strength and density are increased by increasing the cement portion of CSRE and there was a linear relationship between stress and strain in the elastic zone. A nonlinear response was observed before stress reached its ultimate strength, followed by a drop in stress until fracture occurred as shown in Figure 5. Tripura and Singh (2010) specified that the presence of cement is the reason for the nonlinear deformation. They claimed that it is possible to achieve a certain elastic modulus by modifying the percentage of cement in the mix. Their study showed that increasing cement from 0 to 10% increases the compressive strength from 1.1 to 9.73 MPa respectively.

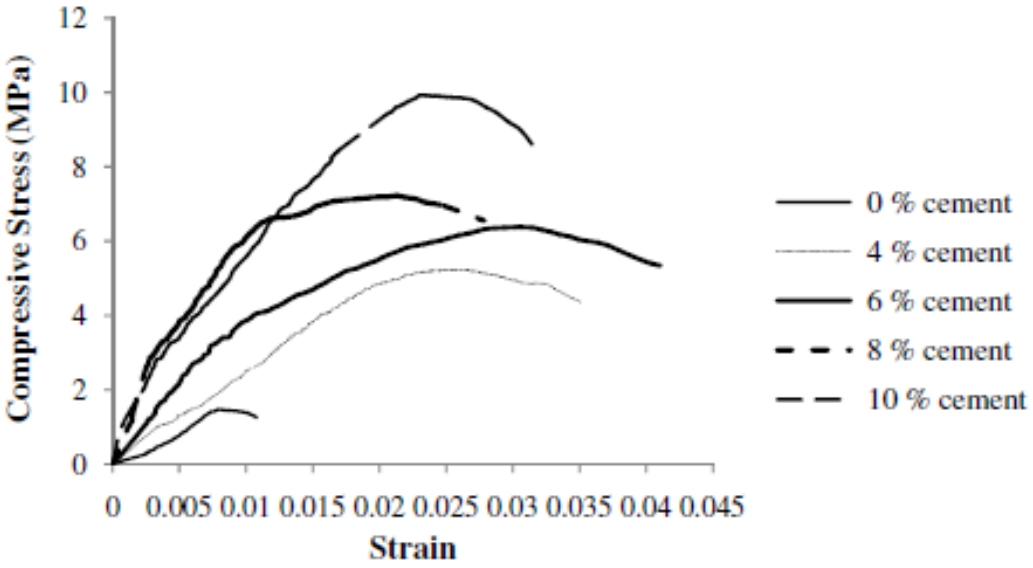

Figure 5: Stress-strain curve of test samples based on various cement ratio Tripura and Singh (2014)

In addition, Tripura and Singh (2014) presented the effect of curing time on the compressive strength of CSRE where they noticed that compressive strength improved as the curing time increased. As Figure 5 shows, they found that compacted soil with 10% cement had a compressive strength of 5.5 MPa after 7 days of curing, however, it climbed to 9.5 MPa when cured for 28 days.

It is important to emphasize from what was mentioned previously, that increasing the cement content ratio increased strength.

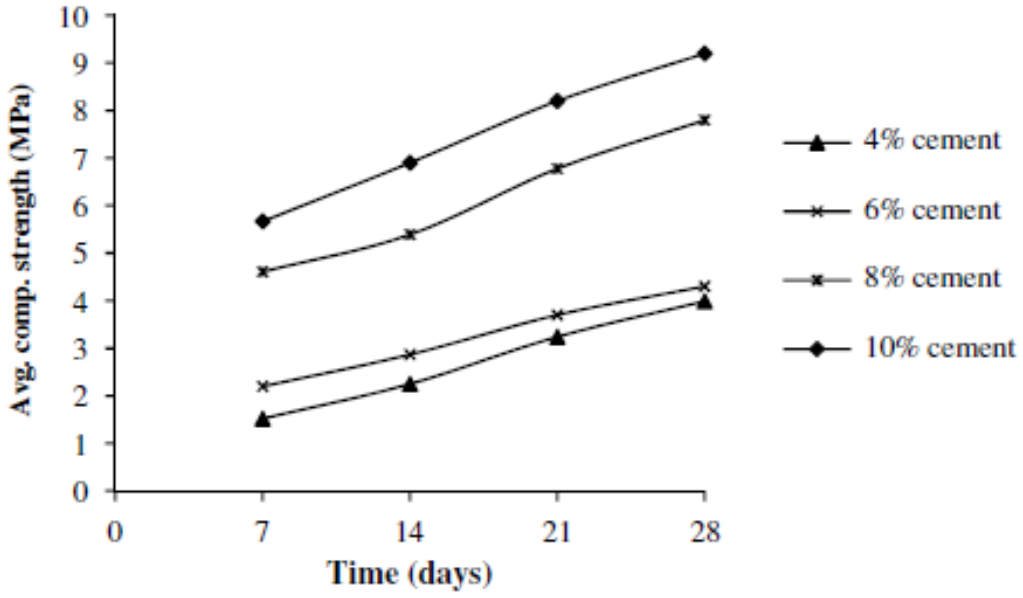

Figure 6 influence of curing time on compressive strength Tripura and Singh (2014)

Tripura and Singh (2014) explained that increasing the compaction energy caused the density to increase, which also increases compressive strength. For example, Figure 6 shows that compressive strength for CSRE went up from 7 MPa to 10.5 MPa when the density increased from 1750 kg/m^3 to 2000 kg/m^3.

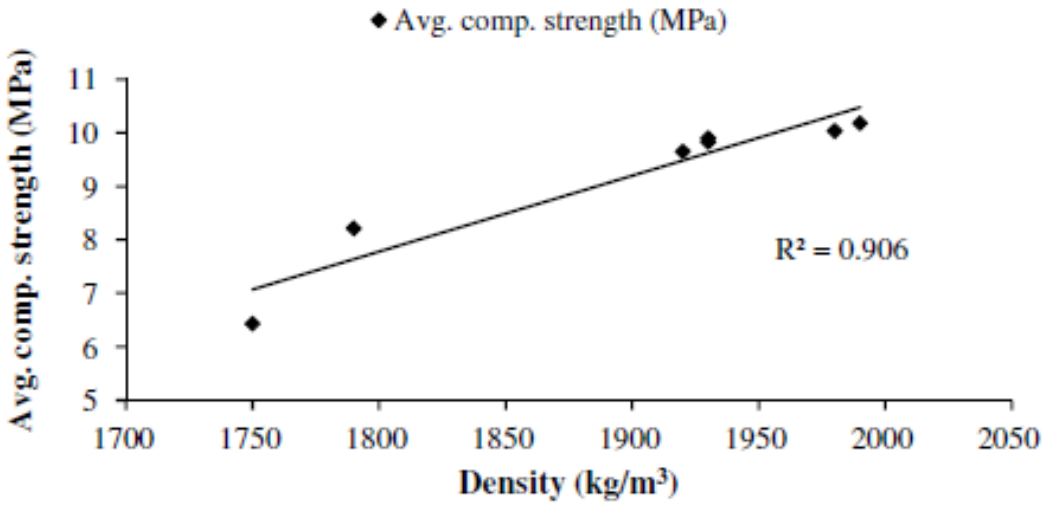

Figure 7: Compressive strength versus density [Tripura and Singh]

Other studies have recommended using locally-sourced materials that are available in large quantities in order to enhance compressive strength as well as the physical and thermal properties of rammed earth systems. For instance, Corbin and Augrade (2014) argued that as an alternative to adding cement, adding wool increases the ultimate compressive strength of CSRE, as Figure 8 shows.

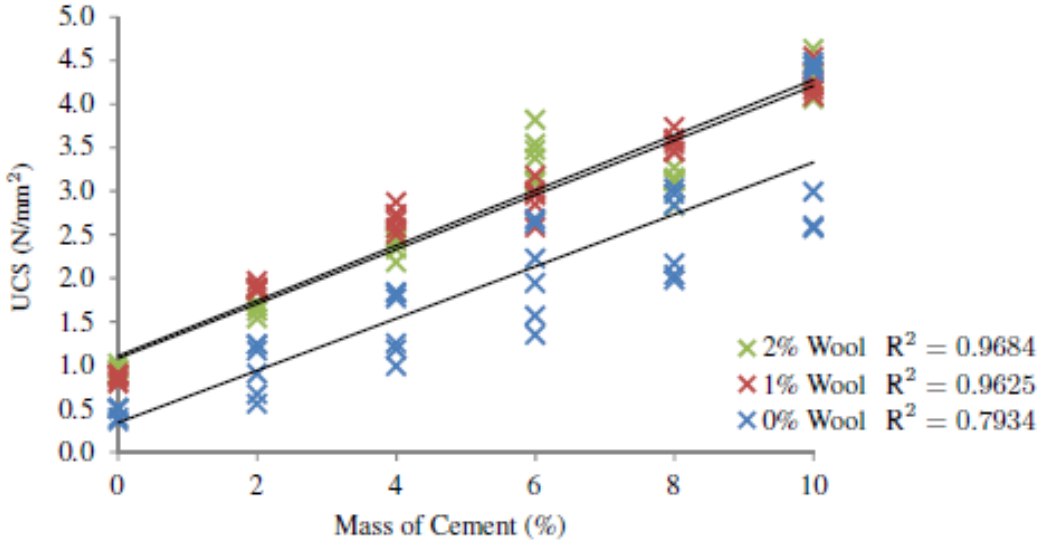

Figure 8: The effect of cement and wool content on ultimate compressive strength by [Corbin and Augrade]

Milani and Labaki (2012) mixed locally-sourced rice hush ash with cement stabilized soil. Their conclusion stated that there was a decline in the thermal conductivity when soil was mixed with rice hush ash compared to cement-soil only which is desirable for insulation purpose. The reason as they argued is that the rice husk ash has more pores than the soil particles. The pores will be filled with air which will not transfer the heat and result in lower thermal conductivity than the soil. They stated that the thermal conductivity for 100% soil stabilized with 10% cement stood at 0.8 W/mK. This figure, However, dropped to 0.65 W/mK when the 92.5% soil was mixed with 7.5% ash and stabilized with 10% cement.

Tang et al (2016), investigated the tensile strength of fiber-reinforced soil and they founded that adding 2% fiber to soil with 1700 kg/m^3 dry density and compacted at 16.5% increased the tensile strength of the soil nearly 52%.

Ma et al (2016). studied the effect of fly ash class (F) on self-compacting rammed earth construction stabilized with cement-based composites (CSCN). They use concrete vibrator to avoid use of compaction energy. They drew a conclusion from the experiment that adding fly ash to CSCN will increase compressive strength and secant modulus. They maintained that the highest strength for the samples with various percentage of CSCN existed when the fly ash content did not exceed CSCN amount.

Ciancio and Robinson (2011) presented in their paper “Use of the Strut-and-Tie Model in the Analysis of Reinforced Cement-Stabilized Rammed Earth Lintels” that the compressive strength of small samples may have a significant difference from big samples. Furthermore, their study suggested that the guidance used in concrete structure design may applied to cement-stabilized rammed earth structural elements.

Finally, only few researchers investigated the elastic modulus cement-stabilized rammed earth. For example, Jayasinghe and Kamaladasa (2006) recommended that the elastic modulus of cement stabilized rammed earth was in range of 500 MPa (72500 psi) which is same value as suggested by The Australian Earth Building Hand Book as they indicated. Moreover, Jayasinghe and Kamaladasa (2006) addressed that moisture content is a cretieria that affect compaction energy and strength of rammed earth wall system. They assert that the moisture content must not be too little nor too high. If the moisture content is too low, the strength will result in low strength and If it is too high the soil will be sticky and will not be compacted well. They recommended using the optimum moisture content

Maniatidis and Walker (2008) found that there is a lack in the experiment data with regard to the modulus of elasticity, so they proposed the value stated in the New Zealand standard which is three hundred times the characteristics compressive strength ($E=300 \times f_c$) or 500MPa as it is in the Australian Earth Building Hand Book.

3. Objective of the study

The objective of this research is to study the effect of adding and using different types of additives on the compressive and flexural strength of soil used in building construction. Different ratios of fly ash, and/or cement were added to the soil to improve the compressive strength and the other characteristic properties of stress-strain diagram. However, recycled fiber materials were used to wrap and reinforce the cement-soil specimens in order to enhance the flexural strength and control the cracks and the mode of failure. The following parameters were considered for the purpose of this study:

- The effect of adding fly ash type C or type F on the compressive strength of soil and soil-cement mix
- The effect of recycled fiber mesh such as polymer or burlap cloth on the flexural strength of cement-soil specimen.
- The effect of glass fiber on the flexural properties of cement-soil beams.

4. Methodology

In this research, series of two types of tests were performed, the first test was a compression test and the second test was a flexural test. Unconfined compression tests were applied to twenty-five cylinders including five samples of soil, five samples of soil with fly ash type C additives, five samples of soil with fly ash F, five samples of soil mixed with cement, and five samples of soil stabilized with cement and fly ash C. Bending tests, however, were conducted using twelve samples of beams. Three beams were made of soil with cement additives only, while the other samples were soil and cement wrapped with materials such as FRP and Burlap cloth. Also beams made of cement-soil material mixed with 2% of glass fiber were prepared.

4.1.Soil Properties

The soil used in these experiments had a red clay and was collected at the depth of 12 feet. Its properties were identified and analyzed before the soil was stabilized with cement and fly ash. The proctor test was conducted to identify the optimum moisture content. Soil content and properties were evaluated using gradation test to determine if the soil type is appropriate for the rammed earth system. According to Barroughs (2008), who tested different types of soils and studied soil properties, linear shrinkage (LS) and the plasticity index (PI) are the primary criteria used for determining the most appropriate soil for rammed earth stabilization. Based on linear shrinkage LS and plasticity index PI values, Barroughs (2008) defined two types of soil, favorable soil with either LS < 6 and PI < 15; or LS from 6 to 11, a PI from 15 to 30 and sand content < 64%. However, unfavorable soil is soil with either LS > 11 and PI > 30; or LS from 6 to 11, a PI between 15 and 30 and sand content > 64%. Below, Figure 9 summarizes Barroughs' findings to determine the soil type. However, Verma and Mehra (1950) used different criteria in their conclusion that a suitable soil for rammed earth system has a sand percentage of a minimum 35% of the soil content,

a Plasticity Index between 8.5 and 10.5, and a Liquid Limit that does not exceed 25%. Easton (1982), another scientist, presented in his study that suitable soil will have 70% sand and 30% clay. In comparing these findings, it can be noticed that when PI is less than 15%, this will be a good indicator about the soil performance. Although these studies disagree on exact sand content, they do agree about sand content should be larger than 35% of the soil content.

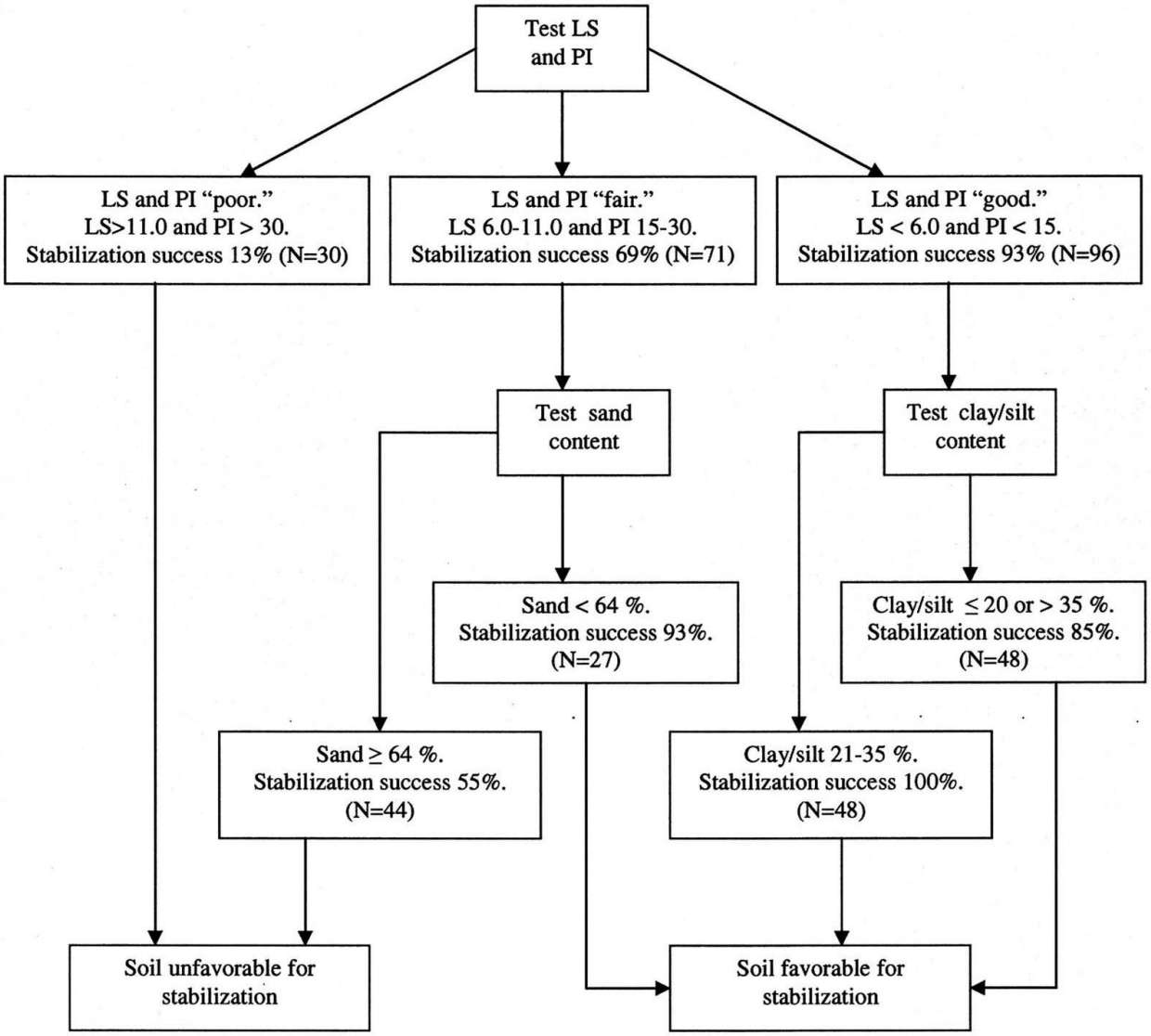

Figure 9: Barroughs procedures for determining soil favorability for stabilization

Soil that was used in this study was evaluated in standard methodology, to determine the optimum moisture content, maximum dry density and other properties such as Liquid Limit, Plastic Limit and Plasticity Index. Then it was compared to criteria defined by Barroughs (2008), Verma and Mehra (1950), and Easton (1982). The properties and composition of soil used in this research were tabulated as shown below in table 1 and table 2.

Table 1 Soil Properties

Maximum dry density	1.83x10-3 kg/cm3
Optimum moisture content	14.1%
Liquid Limit (LL)	27%
Plastic Limit (PL)	16.5%
Plasticity Index (PI)	10.5%

Table 2 Soil Composition

Sieve	Weight [kg]	Sieve and Soil	Soil on Sieve	Cumulative weight	Passing	Percentage Passing
#4	0.525	0.575	0.05	0.05	1.575	97%
#10	0.445	0.675	0.23	0.28	1.345	83%
#40	0.38	1.08	0.7	0.98	0.645	40%
#100	0.36	0.7	0.34	1.32	0.305	19%
#200	0.335	0.355	0.02	1.34	0.285	18%
Pan	0.38	0.665	0.285	1.625		

As it can be seen from table 1, Plasticity Index for the sample is 10.5% which lies within the range define by Veram and Mehra (1950) of 8.5% and 10.5%. Furthermore, this value meet Burroughs criteria which is less than 15%. plastic limit is 16.5% less than 25%. What is more, the table presents that the optimum water percentage required to achieve the maximum dry density is 14.1%. According to Unified Soil Classification System, the soil is classified as SC, sand clay soil. Consequently, the collected soil for this study is considered as a suitable soil for rammed earth system.

4.2.Cylinder preparation

In this investigation, twenty-five cylinders were prepared and grouped in five types with five samples for each type. Each group was mixed with different ratios of soil, ash, and/or cement content to determine the unconfined compressive strength and the catachrestic properties of the stress-strain graph for each type. The following types are listed below:

- Soil only
- Soil with 12% fly ash F
- Soil with 12% fly ash C
- Soil with 12% cement
- Soil with 6% cement and 6% fly ash C

The process entailed drying the soil in an oven, crushing the dried soil back down to its original grain size and mixing it with fly ash and/or cement in ratios listed above. Next water was added to each mixture, filled into a mold and compacted in layers. For more details, the procedure was explained further in the following paragraphs.

The collected soil materials were placed in a clean tray inside a lab oven at a temperature of 220 F for 24 hours to dry completely. After the soil was oven-dried, it was taken out and left about ten minutes to cool down. Then it was crushed in order to return the soil to the original size without breaking the particle itself. The crushed soil was sieved before mixing using pan#4 to ensure there was no unusual size of particle.

Figure 10 Photo of the oven used to dry the soil material

Figure 11 Soil in the crushing machine

Figure 12 Photo shows soil in sieve#4

Using clean tools, soil was mixed with cement and/or fly ash in ratios listed previously until the mix content was uniformly distributed. Next, water was added gradually to the dry mix using spry bottle. Although the optimum moisture content determined by proctor test was 14.1%, the amount of the water used in the experiment was increased to 15% to take into account the water absorbed by the tools and the evaporation during the mix process. Consequently, the mix poured into the PVC mold of 4 in cross sectional diameter and 8 in height. The PVC mold itself was made in two separated semi-cylindrical shapes, and both parts were tied together by steel strips. The mold was then stood upright on a steel base. Next, the inside of the mold was coated with petroleum jelly or DW10 oil to prevent the soil mix from sticking to the PVC mold sides. This was done to make it easier to remove the sample out of the mold and assure the sides of the samples were uniform. The non-uniformity of the samples sides could result in a reduction of unconfined compressive strength.

Figure 13 PVC mold used to prepare the cylinder sample

The soil was poured in the mold in three layers, and each layer was compacted using a proctor test hammer to provide compaction energy and reach its maximum dry density. The number of blows each layer received was 50. When each layer was compacted, its top surface was scratched to provide effective bond with the layer placed above. When compaction is done, the specimen was removed from the mold immediately and left in the lab room for 24 hours. Then the specimen was cured for 28 days inside a curing room before it was moved out to be air-dried for other 14 days.

Figure 14 Hummer used to provide compaction energy

Figure 15 shows photo of the curing room

Figure 16: Cylinder Specimen

An oven-dried method was used to ensure a specimen reaches its maximum dry density. For this purpose, a specimen was weighted after it was removed from the mold and also a small portion of the mix was taken, weighted, and placed in an oven to dry for 24 hours. After a small portion was dried, it was weighted again to determine its water content. The following example shows the procedure to ensure a specimen reaches its maximum dry density.

Wet weight of a small portion	19.9 g
Dry weight of a small portion	17.3 g
Weight of water content	19.7-17.3 = 2.6 g
Water content ratio	2.6/19.9 = 13%
Wet weight of the specimen	3.57 kg

Dry weight of the specimen	3.57/1.13 = 3.16 kg
Volume of specimen	1686.6 cm^3
Calculated dry density of specimen	3.16/1686.6 = 1.87 x 10^{-3} kg/cm^3
Experiment dry density	1.83 x 10^{-3} kg/cm^3

A Comparison between calculated and experimental dry density shows that the specimen reached its maximum dry density of 1.87 x 10^{-3} kg/cm3, which is slightly over experimental dry density, 1.83 x 10^{-3} kg/cm^3.

Before conducting the compression test, the specimen was capped at the top and the bottom by compound material to distribute the compression force over the specimen end surfaces and ensure that the failure will occur in the middle of the sample far from both ends. Finally, the specimen was ready for the compression test.

4.3.Compression Test

The most useful way to present the strength and characteristic of any material is to conduct a compression test and graph a stress-strain diagram. This concept applies to any material regardless of the dimensions of the specimen. Therefore, the compression test was conducted using an Instron machine that produced experimental data results to a connected computer. The specimen was placed between two steel plates to distribute the load over the round surface. The test was load controlled, the load was increased gradually and the response of the specimen was registered for each step of increased load.

Figure 17 Instron machine

4.4.Beams preparation and bending test

A steel mold of 4in x 3in x 16in was used to prepare the beam samples and the span length was larger than three times the depth. There were three types of beams and each type was made of different materials as follows:

- Three beams made of soil mixed with 12% cement
- Three beams made of soil mixed with 12% cement, wrapped by fiber reinforced polymer (FRP) mesh, and reinforced with additional FRP mesh
- Three beams made of soil mixed with 12% cement, wrapped with burlap cloth and also reinforced with an additional layer of burlap

- Beams made of cement-soil and reinforced with 2% (uncompact volume) of fiber glass

Figure 18 Steel mold used in the experiment

4.4.1. Cement-soil beam

For cement-soil beams, the same procedures of the cylinder preparation were followed, but the mix was prepared and compacted in one layer instead of three layers as the height of the beam was 3 inches.

Figure 19: Cement-soil sample

4.4.2. Cement-Soil beam wrapped and reinforced with FRP mesh

After preparing the mix, a half-inch of the beam height was filled with soil-cement mix to provide a good bonding with FRP mesh that will be placed above in a way that wraps the mold. More soil was fed into the mold above the mesh to fill a third height of the beam and place additional mesh of FRP as a reinforcement. Then the cement-soil material was poured to fill the mold and compacted in one layer at the optimum moisture content.

Table 3 Properties of coated fiberglass mesh

Property	Elastic Modulus [psi]	Tensile strength [psi]
Value	250000	4200

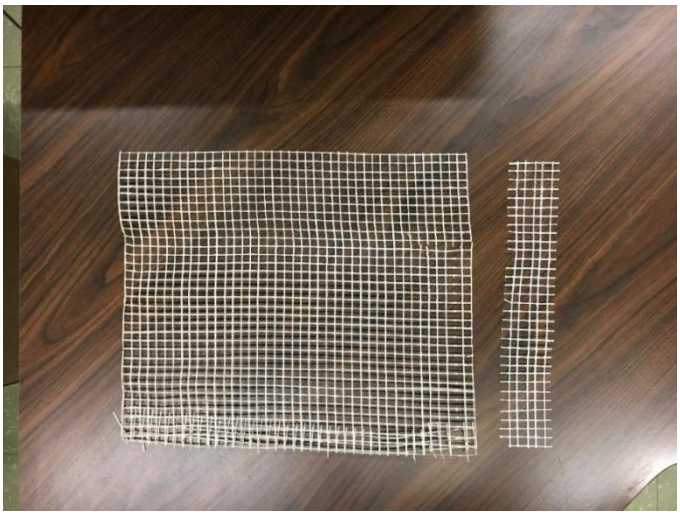

Figure 20 FRP mesh used in the experiment

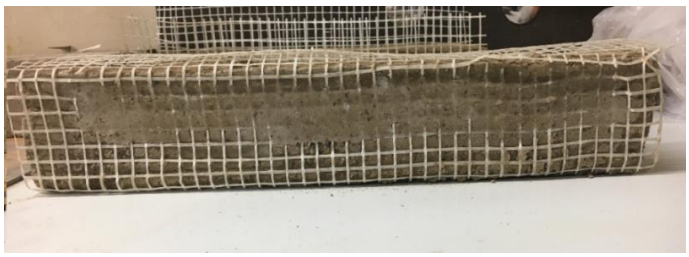

Figure 21 Cement-soil beam wrapped and reinforced with FRP mesh

4.4.3. Cement-soil beam wrapped and reinforced with burlap cloth

Figure 22 Burlap cloth used in the experiment

Table 4 Properties of burlap cloth [Source: Severson (2012)]

	Mass (oz)	Density (oz/in3)	Elastic modulus (psi)
Burlap Cloth	0.81	0.23	353659

As it can be seen from figure 18, two pieces of burlap cloth, recycled jute fiber woven bags, were used and they were sprayed by a water sprayer before the cement-soil material was poured above in order not to absorb the soil water content and to have good bonding with the soil. The big piece of burlap wraps the beam and the small piece is used as a reinforcement layer near the bottom of the beam. First of all, the big piece was placed in a way that wrapped the mold and the cement-soil material was then poured to fill a third of the mold's height. The small piece was laid above the first layer of soil and then more soil was poured into the mold. When it was full, the material was compacted in one layer. Once compaction was completed, the sample was demolded

immediately and kept in the room for 24 hours. One day later, the beam was placed in the curing room for 28 days before being left to dry outside the room.

Figure 23 photo shows how to lay the first piece of burlap cloth

Figure 24 cement-soil beam wrapped and reinforced with burlap cloth

4.4.4. Cement-Soil reinforced with fiber glass

In this type of beam, chopped fiber glass, soil, and cement were dry mixed together until they were uniformly distributed. The fibers were randomly oriented in the mix and its proportion was 2% of the uncompact total volume. It is necessary to mix the fiber with cement and soil before adding water in order to provide uniform distribution of the fiber within the mix. 15% of the water was then added and mixed with the material. The wet mix was poured within a steel mold and compacted in one layer by a standard hummer to achieve the required density of the soil. The prepared beam was removed from the mold immediately, cured, and dried as explained in the cylinder samples.

Figure 25 Mix preparation of cement, soil and fiber glass

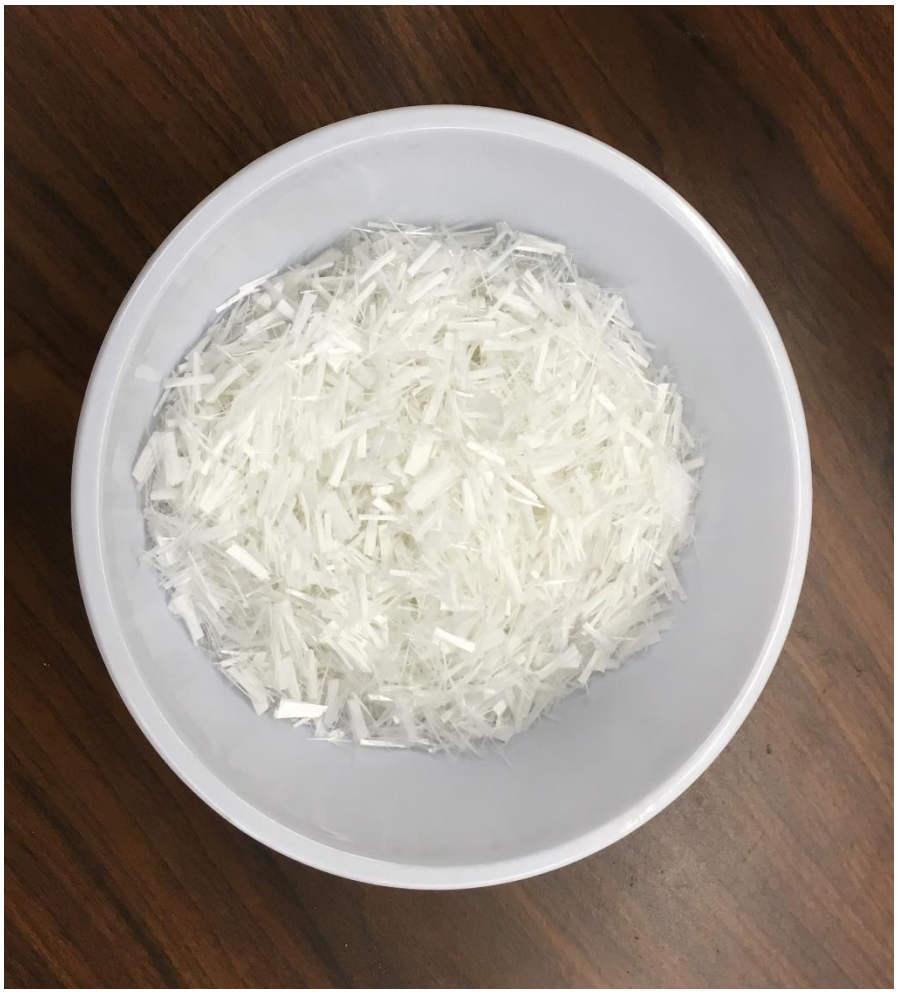

Figure 26 Chopped glass fiber

Table 5 Properties of fibers

Fiber Type	Fiberglass
Density	2500 kg/m^3
Tensile Strength	4000 MPa
Young modulus	80 GPa
Ultimate tensile strain	3%
Poisson’s coefficient	0.22

Figure 27 Cement-soil sample reinforced with fiber glass

4.5.Bending test

The specimen was tested as a simply supported beam under three-point loading. The three-point loading experiment is the most common test for fiber reinforced concrete (based on ASTM Standards and Instron recommendations) and it will be suitable for this study as it measures the post-cracking capacity especially that there are some of the beams are reinforced with fiber and burlap. The beam will be supported on pin supports at the ends and then force at the middle of the beam will be applied at a constant rate using the Instron machine until the sample fractures.

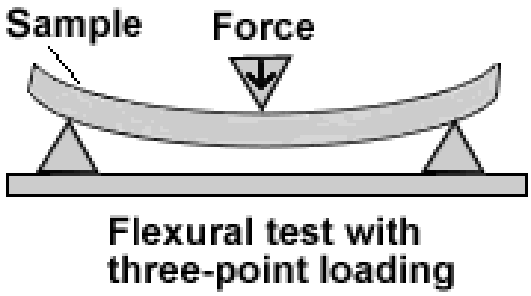

Figure 28 Figure of three-point loading test [Source: Instron website]

4.6.Heat loss Experiment

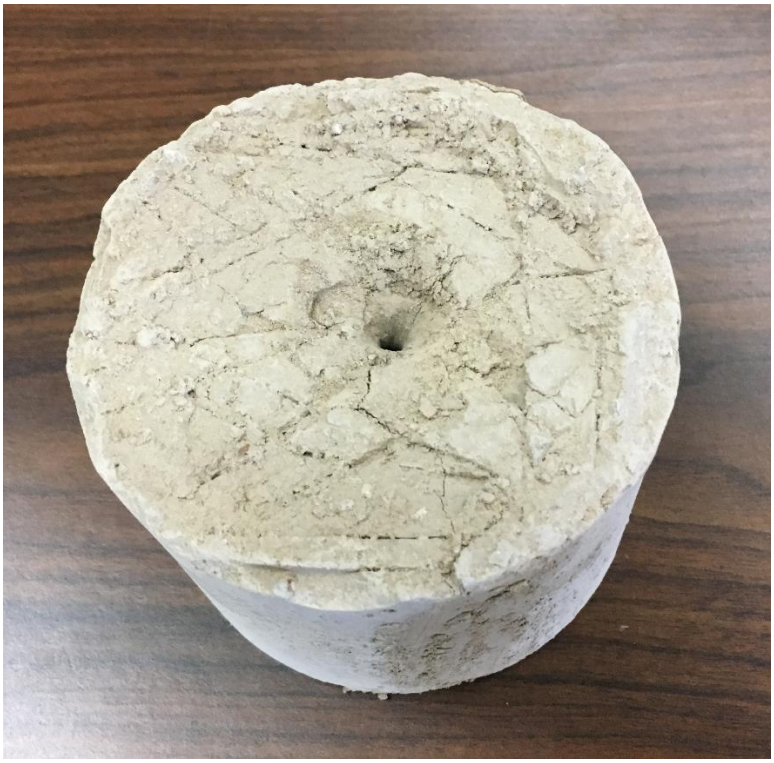

Figure 29 Soil sample to measure inner and outer temperature

One of the soil samples was prepared to measure heat loss and it had a 4 in diameter and 4 in height. A small hole of 2 in deep and 1/8th in in diameter was created at the center of the sample. The sensor was then placed in the hole to measure the inner temperature of the sample as seen in the picture below. The soil sample was heated in a furnace up to 475 F, then taken out and placed on a heat resistant surface to cool down to room temperature. Meanwhile, the temperature of the sample was measured at interval times of ten minutes using a portable digital thermometer to measure the inner temperature by placing the sensor inside the hole. However, a handheld infrared thermometer, efficient for non-contact temperatures, was used to measure the surface temperature of the sample.

Figure 30 furnace picture

Figure 31 Pictures of portable digital thermometer (left) and handheld infrared thermometer (right)

5. Results and discussion

As mentioned previously, two types of experiments, unconfined compression and three-point bending experiments were carried out. Each type has included different types of material, so each type will be discussed in detail in this chapter. Further, comparisons were performed to determine the effect of each type.

5.1.Compression Experiment

In compression tests, load was increased from zero to failure point. Each length reduction due to compression force was registered for each increment of the load. Load and length reduction data were converted to a stress-strain diagram that shows the strength and material characteristic for each specimen. In the following pages, a compression test result of each type will be investigated and presented in graphs before a comparison between the different types was made.

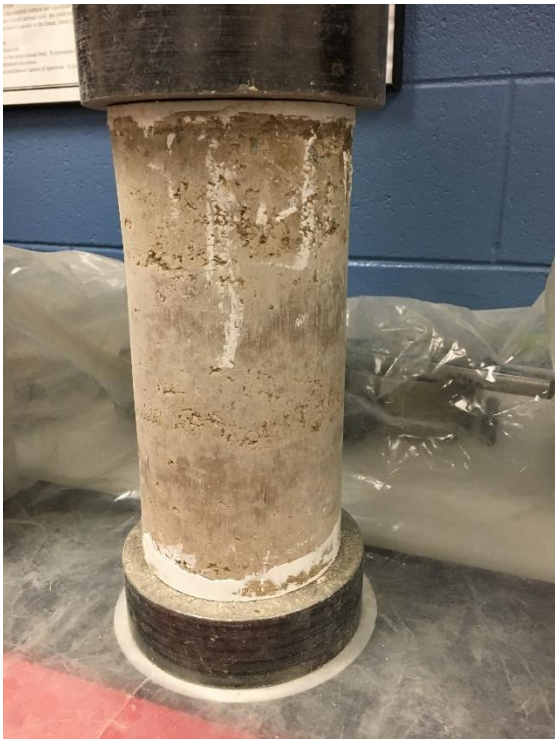

Figure 32 photo of a compression specimen

5.1.1. Soil sample

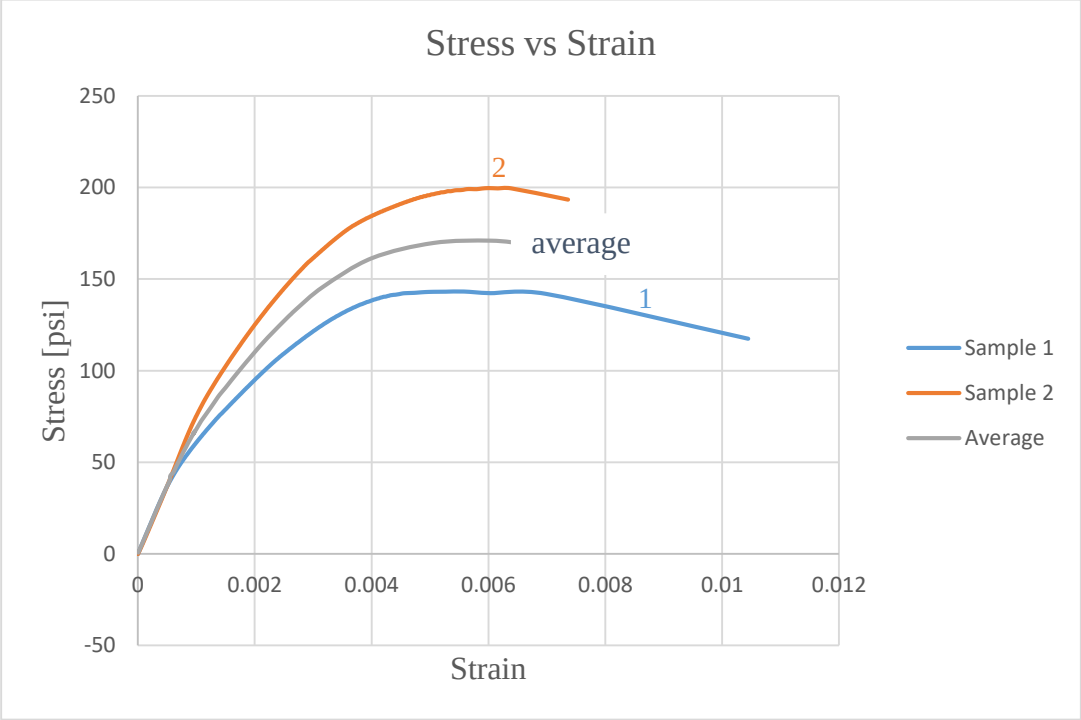

Figure 33 Stress-Strain for samples made of soil only

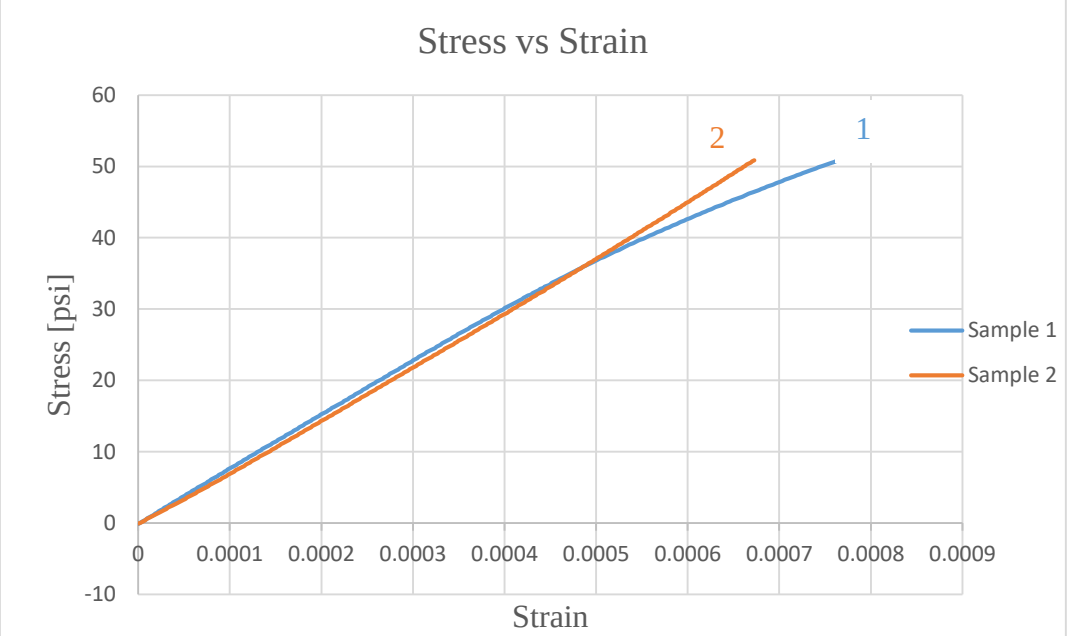

Figure 34 Large scale of stress-strain diagram to show the elastic portion

Figures 33 and 34 illustrate the stress-strain diagram and the characteristic properties of soil samples. Two soil samples were selected to represent the stress-strain diagram. As the applied load to both samples is increased, stress and strain were increased linearly until the stress reached the proportional limit at 50 psi. Within this region, soil material was elastic and no permanent deformation occurred. When the load was increased beyond the elastic limit, the stress applied to the first sample hit the ultimate value at 145 psi before it was decreased and failure occurred at stress of 117 psi. Although the second sample shared the same elastic portion as the first sample, the maximum strength of the second sample was higher than the first sample and stood at 200 psi before it failed at 193 psi. Furthermore, the yield stress was defined as a stress that developed a permanent set of 0.2% stain. A line was drawn from the strain axis at 0.2% set parallel to the elastic line of the stress-strain graph and the intersection point of this line with the stress-strain diagram defined the yield stress. It was 145 psi and 200 psi for the first and second sample respectively and these values matched the maximum strength for each sample. Another material characteristic to mention is the elastic modulus which is measured by the slope of stress-strain curve within the elastic portion. It was concluded that both samples had an elastic modulus of 78000 psi. Although the elastic modulus was high, the elastic portion was small compared with the whole graph and the elastic limit stood around 50 psi which was 35% and 25% of the maximum strength for the first and second sample respectively. Looking at figure 32, the modulus of resilience was almost the same for each sample. For example, the resilience modulus was determined by calculating the area under the straight line in the elastic region of the stress-strain diagram.

MR = 0.5* 50 * 0.00066 = 0.0165 psi

In the following table, the mechanical properties of the soil samples were tabulated:

Table 6 The characteristic properties of soil samples

Material	Soil sample 1	Soil sample 2
Elastic Limit [psi]	40	50
Yield Strength [psi]	145	200
Ultimate strength [psi]	145	200
Modulus of Elasticity [psi]	78000	80000
Modulus of Resilience [psi]	0.012	0.0165

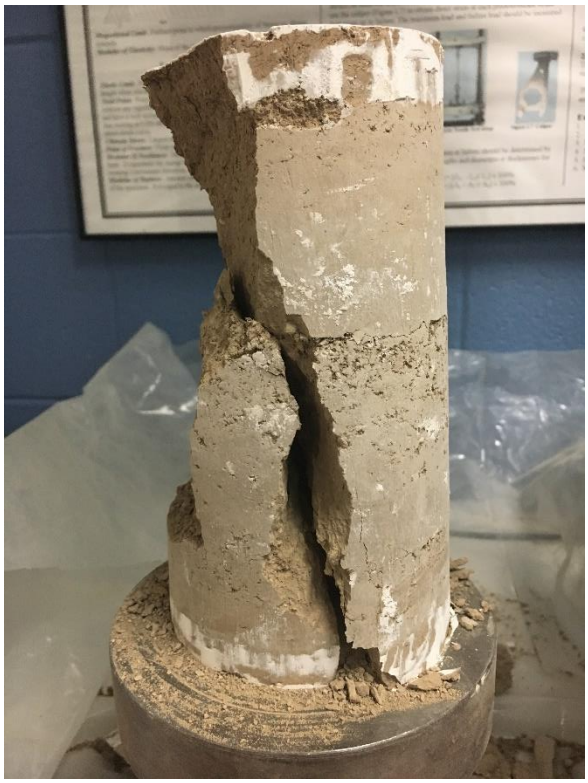

Figure 35 Photo of the specimen after fracture

Figure 34 shows the type of fracture the soil specimen experienced when it was crushed. The type of cracks and failure show a shear failure due to compression force.

5.1.2. Soil with 12% fly ash F

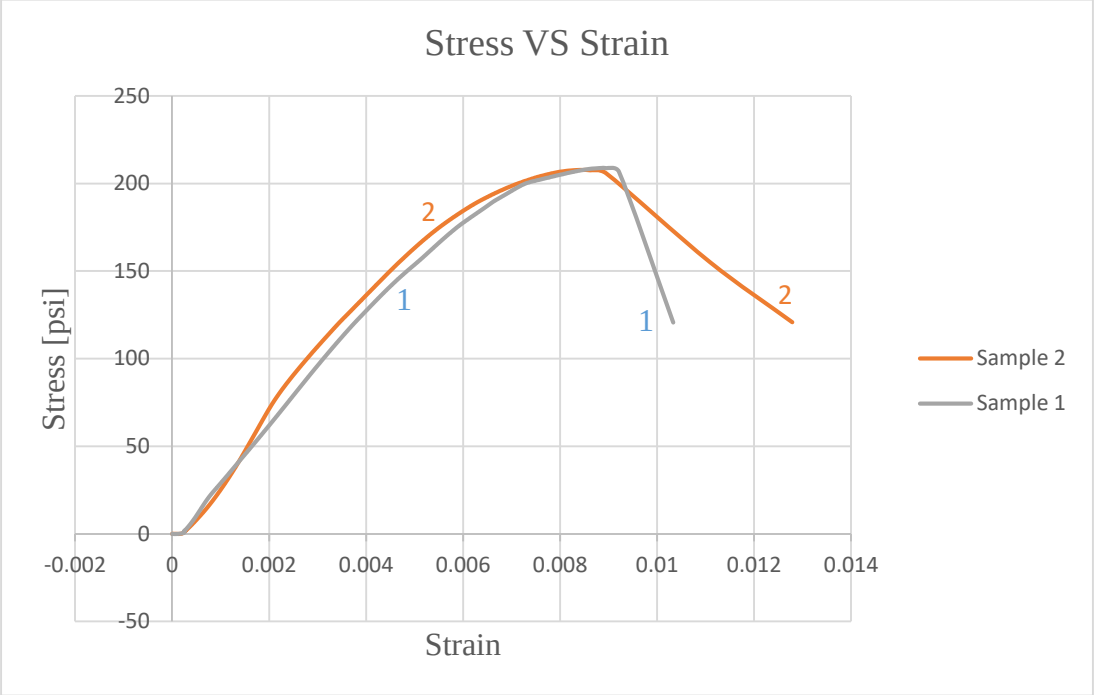

Figure 36 Stress vs Strain for soil-fly ash F

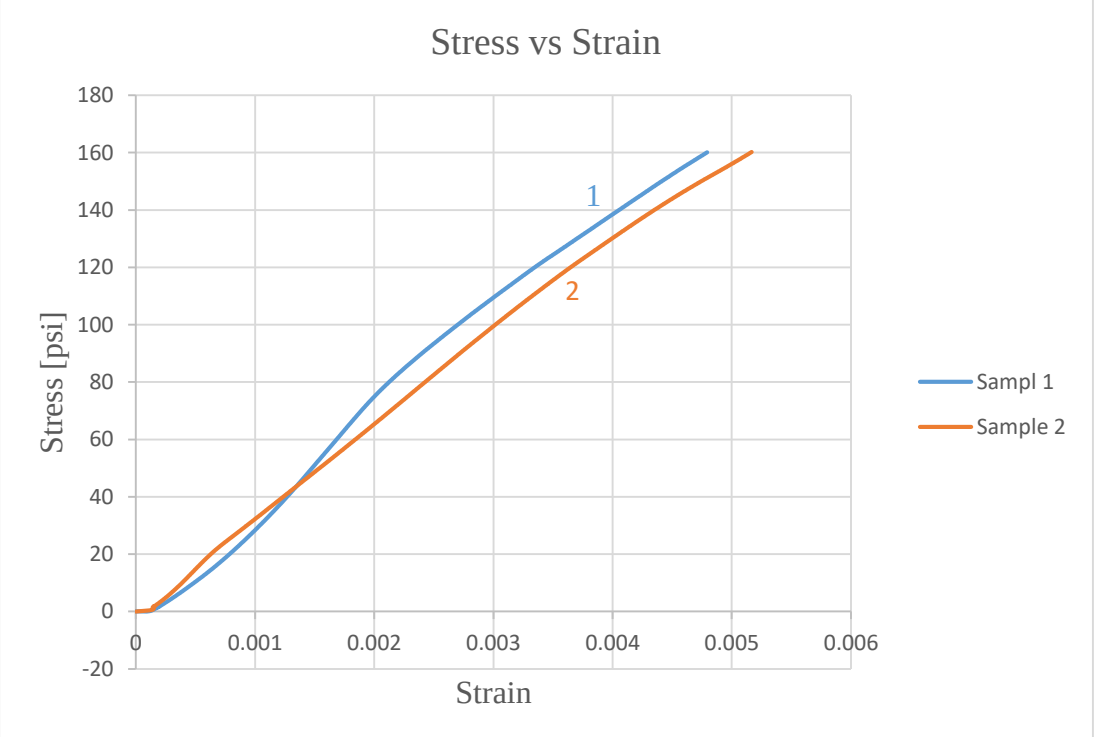

Figure 37 Stress vs Strain in the elastic region for soil with 12% fly ash F

Figure 36 presents the stress-strain graph for two samples to define the mechanical properties of samples made of soil mixed with 12% fly ash F. For both samples, it showed that there was an increase in both stress and strain when an applied load was increased. The stress hit the ultimate strength at 210 psi when the strain stood at 0.009 before sample 1 and sample 2 failed suddenly without warning. Furthermore, the proportional limit of this type of sample was close to the ultimate strength as there is no yielding plateau in the stress-strain graph. Therefore, the modulus of resilience is equal to whole area under the stress-strain graph and it is equal to 0.8 psi. In fact, it is a small value and it indicates that the maximum energy absorbed up to the elastic limit without creating permanent deformation is small.

Figure 37 shows that the stress-strain diagram for both samples have a similar slope when stress is linearly related to strain and the modulus of elasticity is expected to be the same. The average slope calculated for the first sample is 37000 psi, however it is 34000 psi for the second sample.

Table 7 The characteristic properties of soil mixed with 12% fly ash samples

Material	Sample 1	Sample 2
Proportional Limit [psi]	180	179
Yield Strength [psi]	-	-
Ultimate strength [psi]	210	210
Modulus of Elasticity [psi]	37000	34000
Modulus of Resilience [psi]	0.7	0.8

Figure 38 Shear failure of soil with 12% fly ash F

5.1.3. Soil with 12% flay ash C

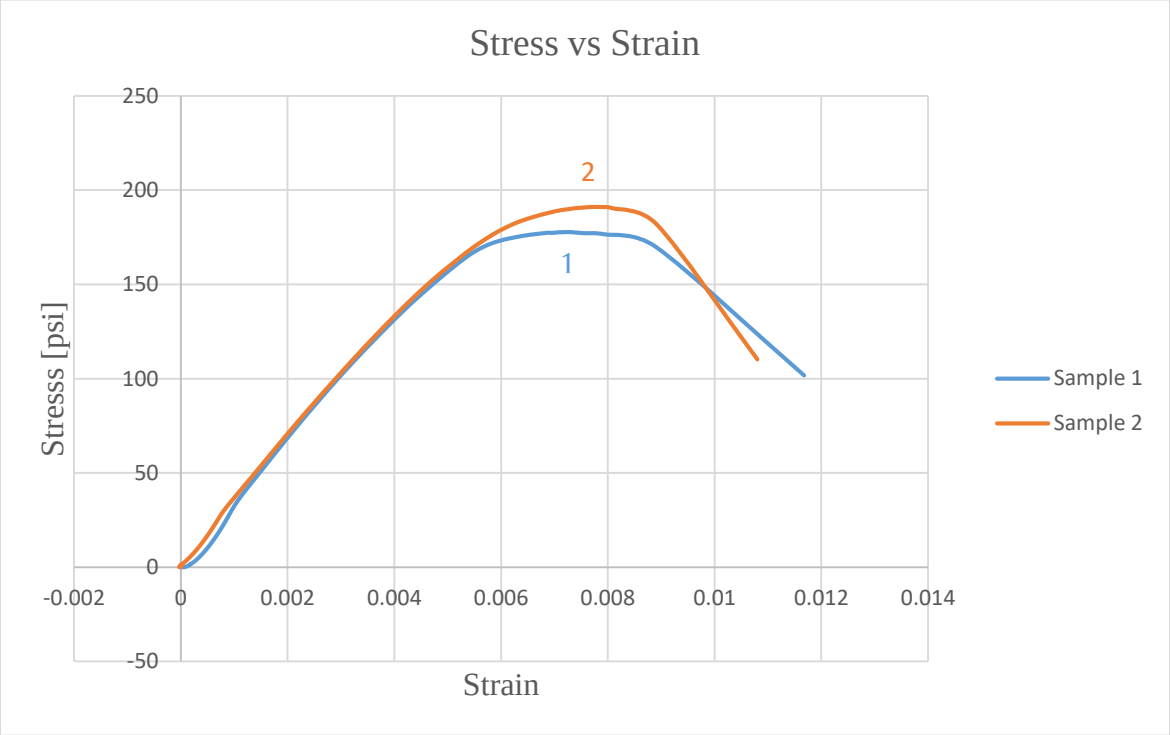

Figure 39 Stress vs Strain for Soil mixed with 12% fly ash C

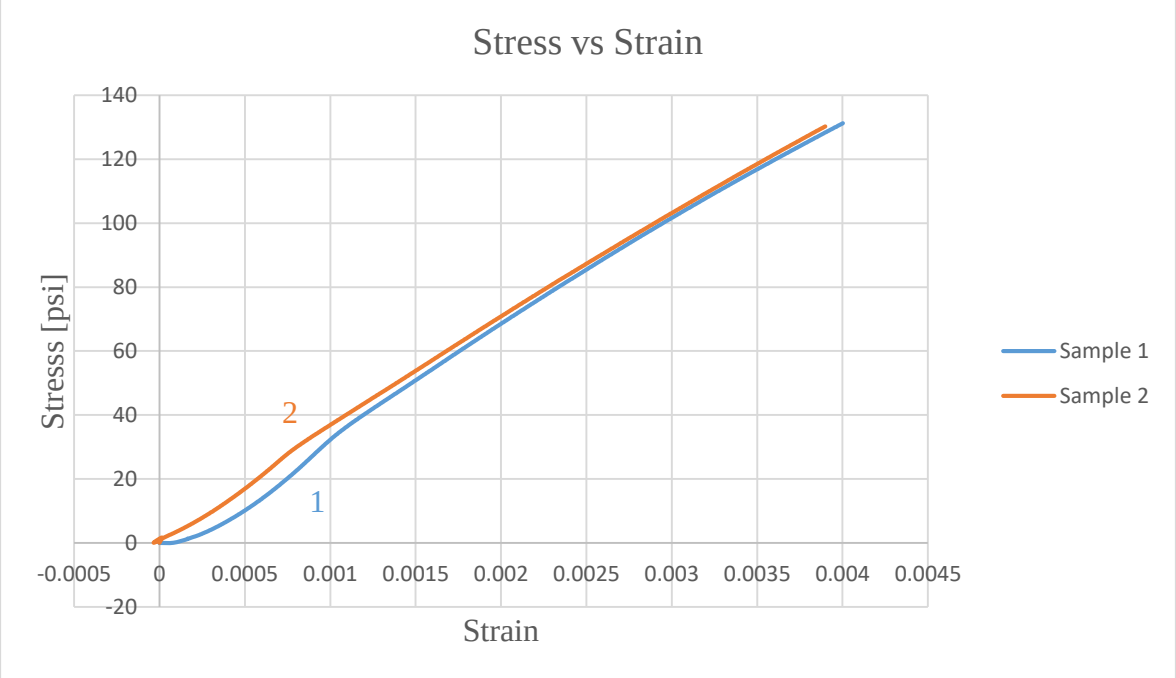

Figure 40 Elastic stress-strain graph for soil with fly ash C

In this section, the characteristic properties of samples made of soil mixed with 12% fly ash C are discussed. When applying load to the samples made of soil and 12% fly ash, they behave exactly the same with only small differences. As it can be seen from the figures above, stress increases linearly with strain before stress reaches the proportional limit at 150 psi. Then, the stress of the first sample rises to reach the ultimate strength of 191 psi when the strain is 0.008, while the stress of the second sample goes up to 177 psi. Next, the stress tends to degrade and failure occurs when strain is around 0.15. The proportion limit reaches 78% and 82% of the ultimate strength for the first and second sample respectively. Yield stress are defined based on 2% set so it is 177 psi and 191 psi for the first and second samples respectively which are the same values of the ultimate strength. On the other hand, the stress-strain graph for each sample in the elastic portion lies over each other and Young's modulus is about 33000 psi for both samples. The following table shows the characteristic properties of samples made of soil and 12% fly ash C.

Table 8 The characteristic properties of sample made of soil and 12% fly ash C

Material	sample 1	sample 2
Proportional Limit [psi]	145	150
Yield Strength [psi]	177	191
Ultimate strength [psi]	177	191
Modulus of Elasticity [psi]	33000	33000
Modulus of Resilience [psi]	0.26	0.26

Figure 41 Shear failure of soil with 12% fly ash C

5.1.4. Soil with 6% cement and 6% flay ash C

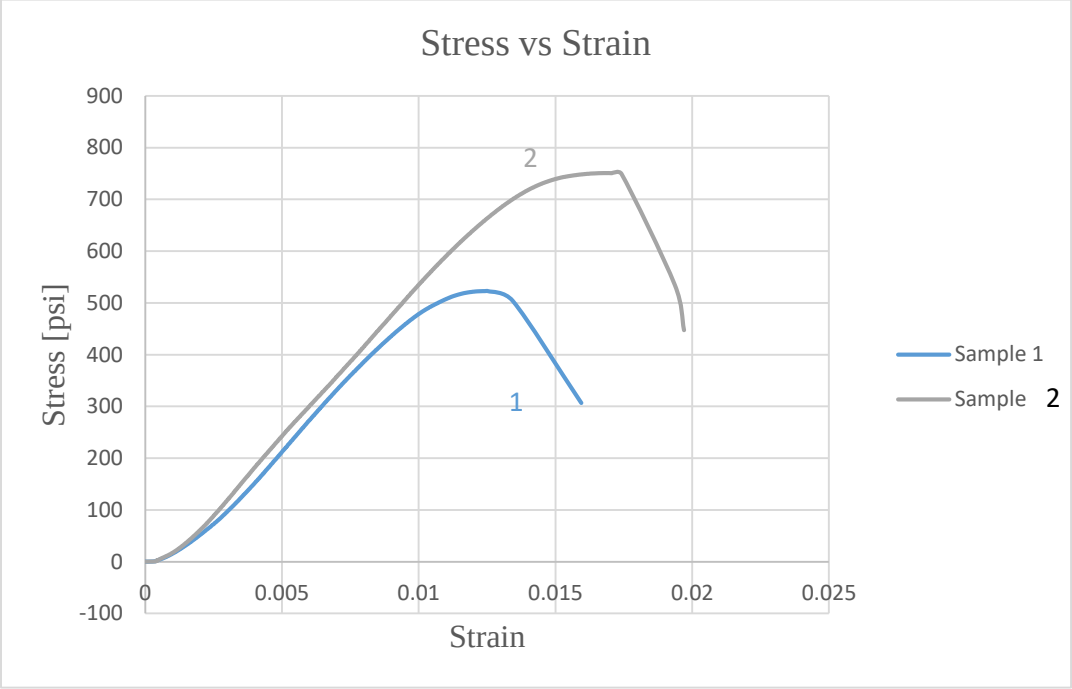

Figure 42 Stress-strain graph for soil mixed with 6% cement and 6% fly ash C

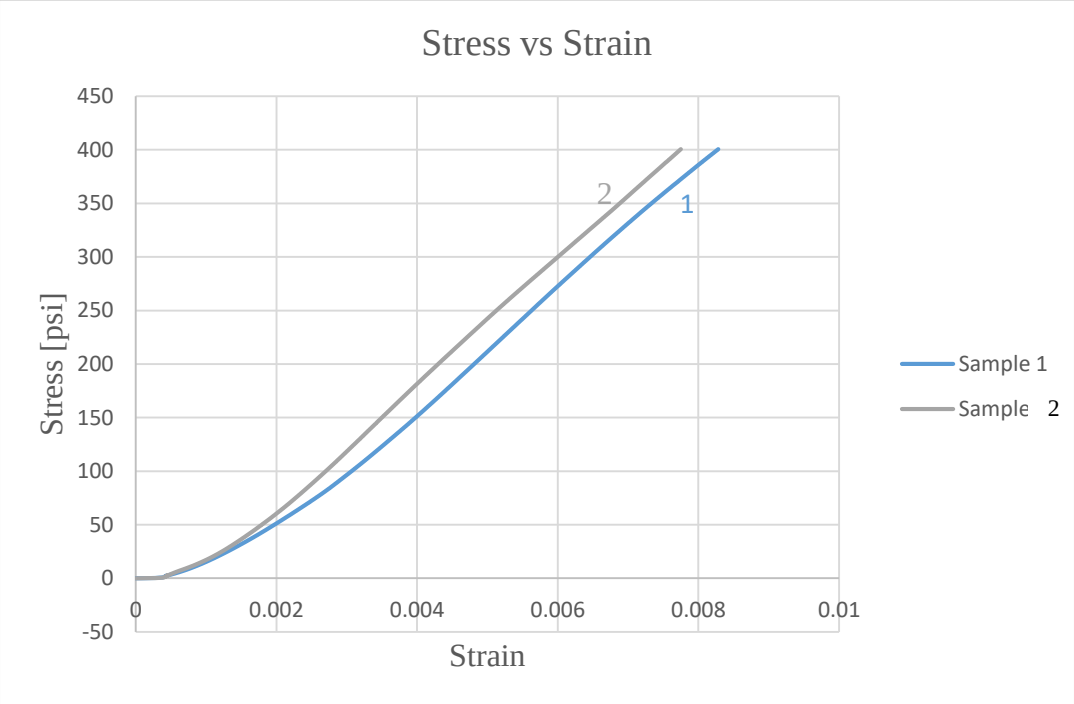

Figure 43 Stress vs Strain in the elastic region for soil with 12% fly ash F

In this test, stress goes up from zero to the proportional limit that stands at 400 psi, before the stress-strain diagram start to curve. Following this stage, the stress rises again to the highest value, 533 psi that represents the ultimate strength before the curve falls to the fracture point. One point to mention is that the proportional limit is 76% of the ultimate strength. Moreover, there is no clear yield point. Furthermore, the modulus of elasticity is calculated based on the slope of the linear portion and it is 60000 psi. Compared to the first sample, the stress-strain diagram of the second sample is parallel to the first sample graph in the elastic region, hence it has the same modulus of elasticity. In fact, it was measured and it was 60427 psi which is close to the 60000 psi corresponding to the first diagram. The difference between the two graphs is that the second sample has an ultimate strength that is higher than the ultimate strength of the first sample. For example, the maximum strength of the second sample is 750 psi which is 43% higher than the first sample although the other properties are the same. Hence, the average of the ultimate strength is 636 psi. The strains at the fracture are 0.0159 for the first sample and 0.0197 for the second sample. Finally, the resilience modulus of the first sample is 1.6 psi. However, the second sample has a resilience modulus of 2.7 psi.

Table 9 The characteristic properties of sample made of soil, 6% cement, and 6% fly ash C

Material	sample 1	sample 2	Average
Proportional Limit [psi]	400	533	467
Yield Strength [psi]	620	730	675
Ultimate strength [psi]	636	750	693
Modulus of Elasticity [psi]	60000	60427	60213
Modulus of Resilience [psi]	1.6	2.7	2.15

Figure 44 Shear failure of sample made of soil, 6% cement, and 6% fly ash C

5.1.5. Soil with 12% cement

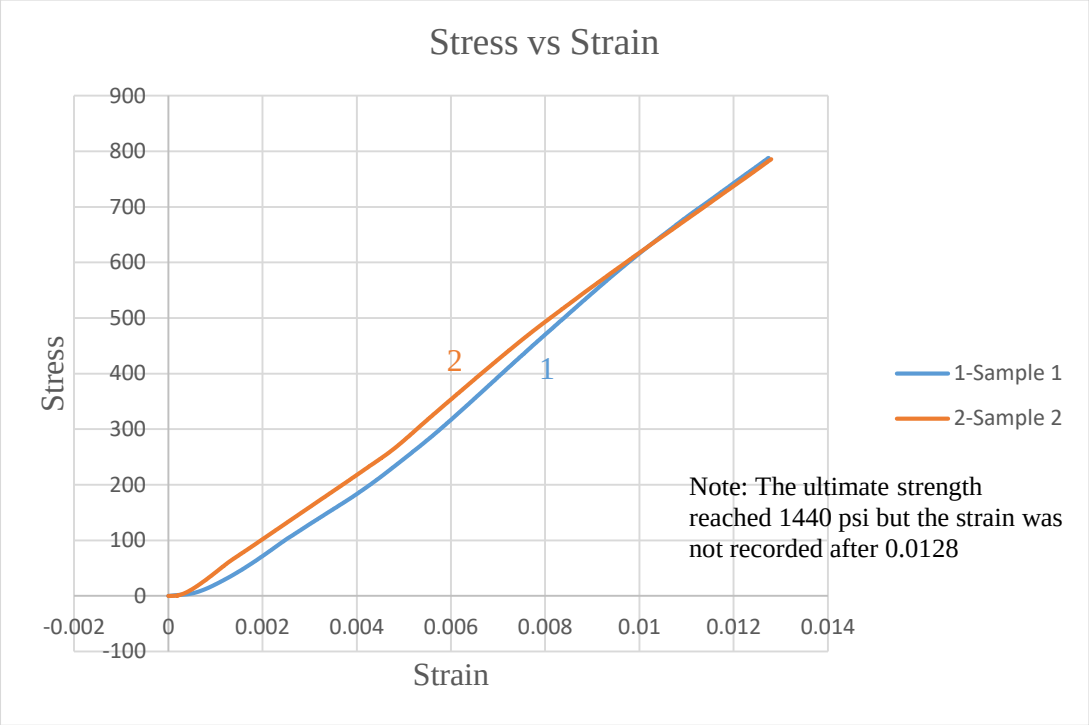

Figure 45 Stress vs Strain for sample made of soil and 12% cement

Table 10 The characteristic properties of sample made of soil and 12% cement

Material	sample 2	Sample 3	Average
Yield Strength [psi]	1400	1400	1400
Ultimate strength [psi]	1472	1420	1446
Modulus of Elasticity [psi]	75000	67000	71000

Table 8 and figure 45 present the characteristic properties of specimens made of soil mixed with 12% cement. It is observed that the ultimate strength of the first and the second specimens are 1472 psi and 1420 psi respectively. The yield strength is not shown clearly and it is nearly 1400 psi for both specimens. Furthermore, the elastic modulus of the first and second samples are 75000 are 67000 psi respectively, so the average modulus of elasticity of both samples is 71000 psi (490 MPa). The average value is close to 500 MPa which is recommended in the Australian Earth Building Hand book. Moreover, the specimen experienced a shear failure at the fracture point as it is seen in figure 45.

Figure 46 failure crack of a sample made of soil and 12% cement

5.1.6. Comparison between the mechanical properties of different types of mix

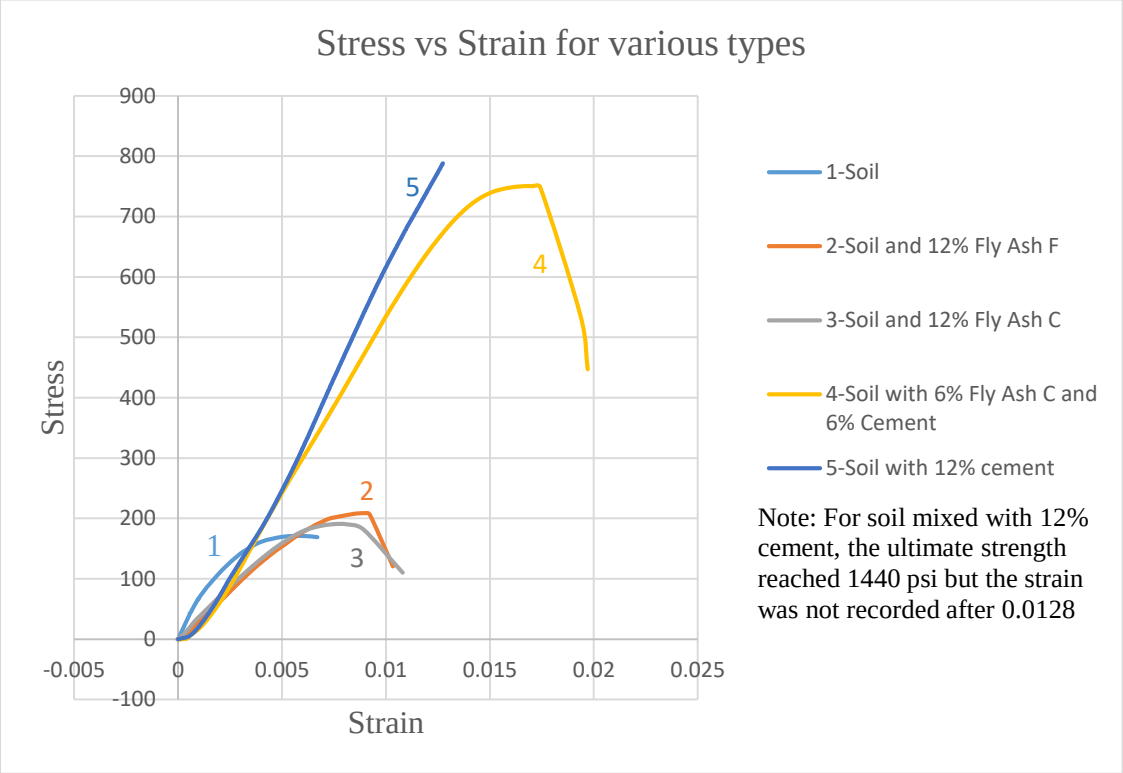

Figure 47 Stress-strain diagram for different ratio of soil mix content

Table 11 The characteristic properties of different ratios of soil mix contetnt

Specimen	Ultimate Strength [psi]	Elastic Modulus [psi]
Soil	171	79000
Soil-12% fly ash F	210	35500
Soil-12% fly ash C	185	35000
Soil-6% fly ash C- 6% Cement	690	60000
Soil- 12% Cement	1445	71000

Figure 47 and table 9 address the characteristic properties of five types of mixed samples, namely soil, soil with 12% fly ash F, soil with 12% fly ash C, soil with 6% fly ash C and 6%

cement, and finally soil with 12% cement. As can be seen from the table, both specimens, soil and soil with 12% cement have the maximum elastic modulus of 79000 psi and 71000 psi respectively. This value drops dramatically by 50% to 35000 psi when the soil is mixed with fly ash C or F. Moreover, specimens made of soil mixed with 6% flay ash C and 6% cement has an elastic modulus of 60000 psi. Therefore, it can be concluded that adding fly ash to soil sample results in elastic modulus reduction as fly ash additives can create voids inside the compacted samples. While a sample made of soil has an ultimate compressive strength of 171 psi, it increases to 1450 psi when 12% cement is added, therefore, adding cement to soil has significant effect on the soil strength, and it causes a remarkable growth in the strength. On the other side, it is concluded from the table and graph that adding fly ash only to soil does not affect the strength. It remains similar to specimens made of soil only. For instance, the ultimate strength of both types of compacted samples, soil only or soil mixed with fly ash, is between 171 psi and 210 psi. The ultimate strength of soil mixed with 6% fly ash and 6% cement falls in the middle place between the soil samples and soil-stabilized with 12% cement. It nearly reaches 700 psi which is 50% less than ultimate strength of sample stabilized with 12% cement.

Another comparison is made in this chapter between the highest ultimate strength specimen, soil stabilized with 12% cement, and a normal concrete sample that has a compressive strength f'_c of 4000 psi at 28 days. The concrete modulus of elasticity is calculated by the equation:

$$Ec = 33 w_c^{1.5} \sqrt{f'}$$

f'_c is the compressive strength f'_c psi at 28 days

Wc is normal concrete weight = 145 lb/ft^3

$E = 33 * 145^{1.5} \sqrt{4000} = 3645000$ psi.

The ultimate strength was obtained from an experiment conducted on a concrete cylinder. To view a comparison, some of characteristic properties of concrete and soil stabilized with 12% cement are tabulated in the table below:

Table 12 Some characteristic properties of concrete and soil stabilized with 12% cement

Sample	Ultimate Strength [psi]	Elastic Modulus [psi]
Soil stabilized with 12% cement	1450	71000
Concrete	5500	3645000

Table 10 illustrates a comparison between the ultimate strength and elastic modulus of concrete and soil stabilized with 12% cement. As it can be seen, the concrete compressive strength is 5500 psi and it is three times larger than compressive strength of cement-soil samples that hit 1450 psi. Moreover, the Young's modulus of concrete is 3645000 psi which is 50 times larger than the elastic modulus of soil samples stabilized with 12% cement.

5.2.Flexural Tests Results

When a load acts at the middle of a simply supported beam, it will bend the beam and this bending will increase as the load increases. Therefore, the maximum moment and deflection will occur in the middle of the span. Due to the beam bending, the beam fiber will be stressed and the stress will increase as it goes far from the cantorial axis toward the outermost fiber. The maximum stress, flexural strength, in the outermost fiber is determined by applying the bending formula. The maximum fiber stress and maximum strain are calculated for the load increment.

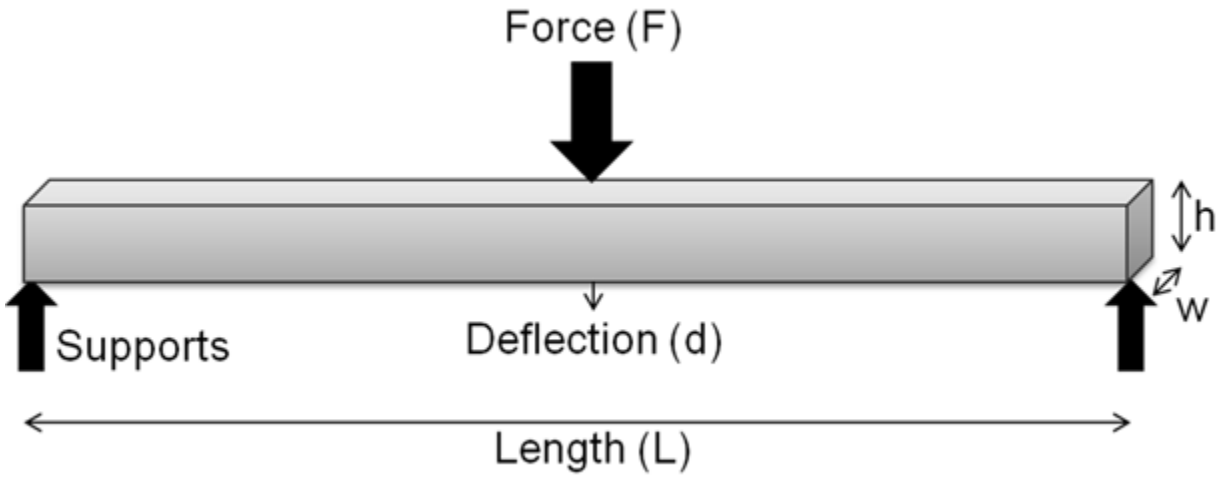

Figure 48 Simply supported beam loaded at the middle (Wikipedia)

$$\sigma = \frac{M\,Y}{I}$$

$$\varepsilon_f = \frac{6\,d\,h}{L^2}$$

E_f = the flexural modulus of elasticity

In the following pages, four types of beams will be discussed:

- Beams made of soil mixed with 12% cement
- Beams made of soil mixed with 12% cement, wrapped and reinforced with FRP mesh
- Beams made of soil mixed with 12% cement, wrapped and reinforced with burlap cloth
- Beams made of soil mixed with 12% cement and 2% fiber glass of uncompact volume

5.2.1. Beams made of soil mixed with 12% cement

Bending tests were carried out on three beams made of soil and 12% cement. Load-deflection and stress-strain diagrams were graphed to comment on the results.

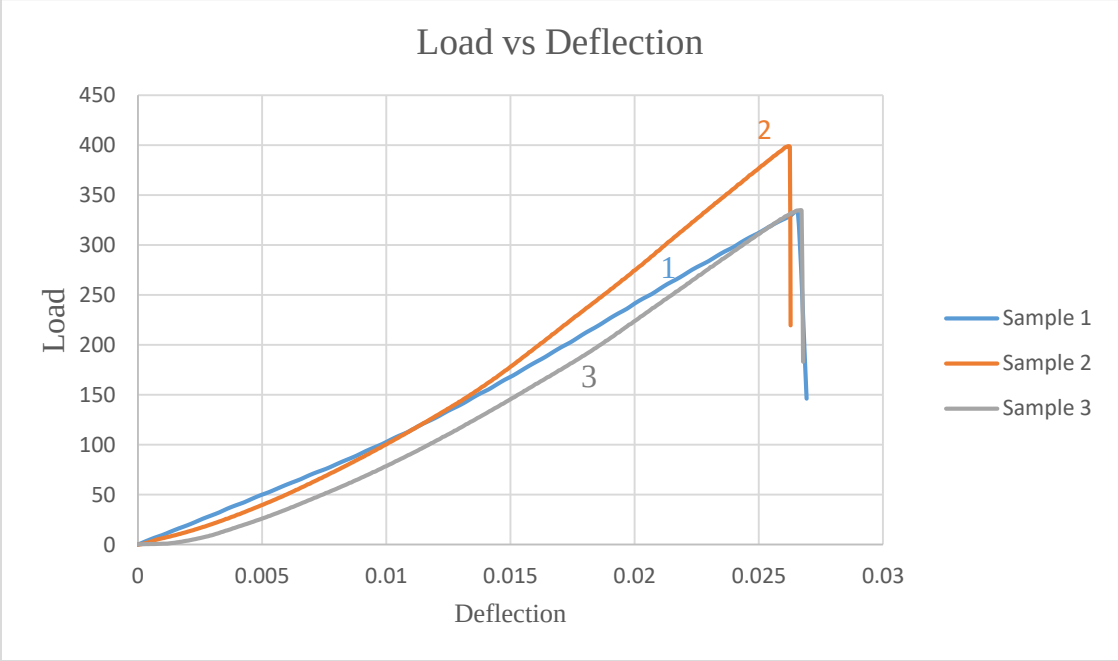

Figure 49 Load-Deflection graphs for beam samples made of soil and 12% cement

As seen from figure 50, all of the three samples did not experience any plastic behavior, instead the load increased linearly with the deflection until fracture. Beams failed without warning at average maximum Load of 360 Ilb. Fracture strains of all samples were close with an average value of 0.00243, while the maximum deflection of beams were around 0.027 in. In addition, the flexural modulus of all beams were defined and it was registered that the second beam had the highest value of 90000 psi and the third beam came in the next place with 78000 psi, then the first beam with 70000 psi. The average value of the flexural modulus was 80000 psi which was close to the number obtained from compression experiments. Finally, failure started when a crack formed due to the tension that occurred at the bottom side of the beam, then it extended up throughout the beam thickness until the beams fractured as seen in the picture 52.

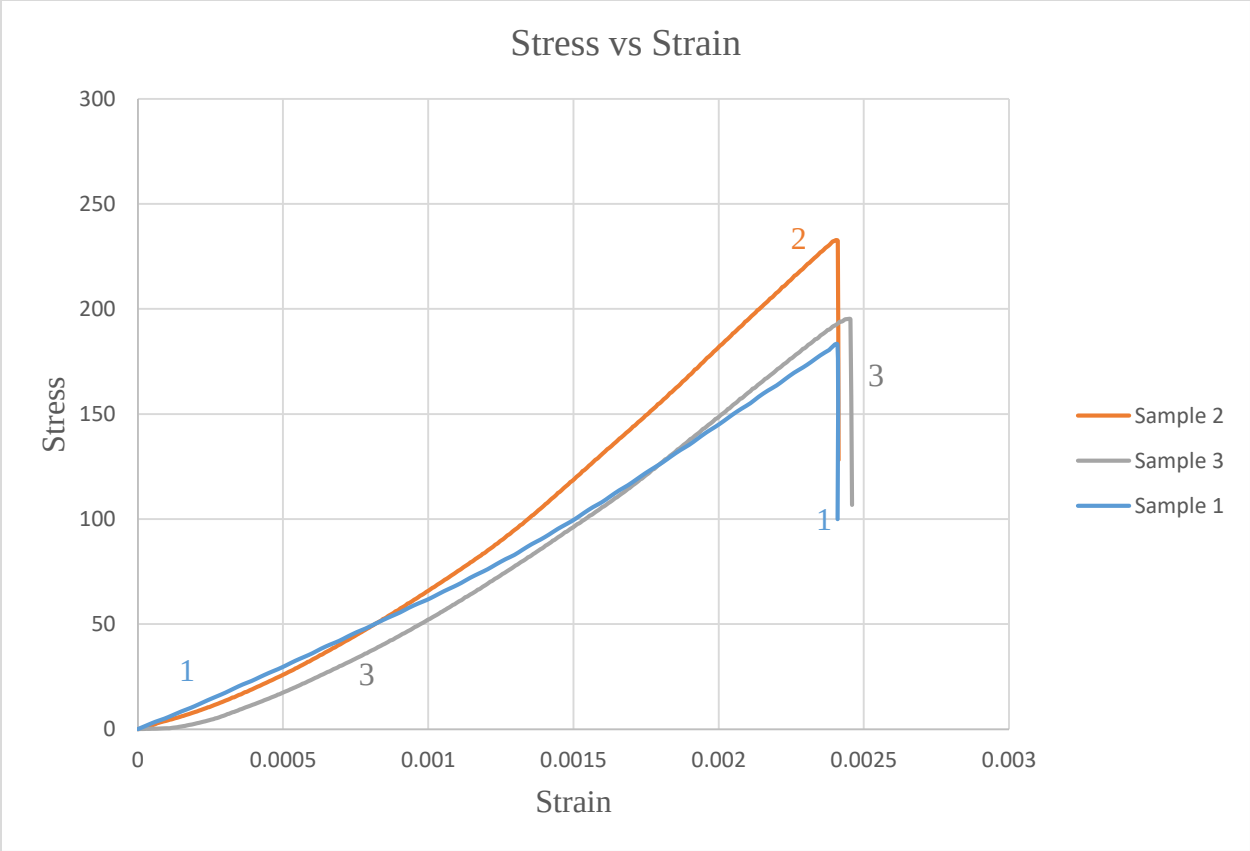

Figure 50 Stress vs Strain for beam made of soil and 12% cement

Table 13 Summary of characteristic properties of beams made of soil and 12% cement

Sample #	1	2	3	Average
Max. Load (lbf)	335	400	335	360
Deflection at Max Load (in)	0.0268	0.02628	0.0268	0.0266
Max. stress (psi)	185	233	195	205
Strain at max Stress	0.0024	0.00241	0.00245	0.0024
Flexural modulus (psi)	70000	90000	78000	80000

Figure 51 Tension fracture of a beam made of soil with 12% cement

5.2.2. Beams made of soil mixed with 12% cement, wrapped and reinforced with FRP mesh

In this section, three experiments were conducted on beams made of soil and 12% cement which were then wrapped and reinforced with fiber reinforced polymer (FRP). Load-deflection and stress-strain diagrams were analyzed.

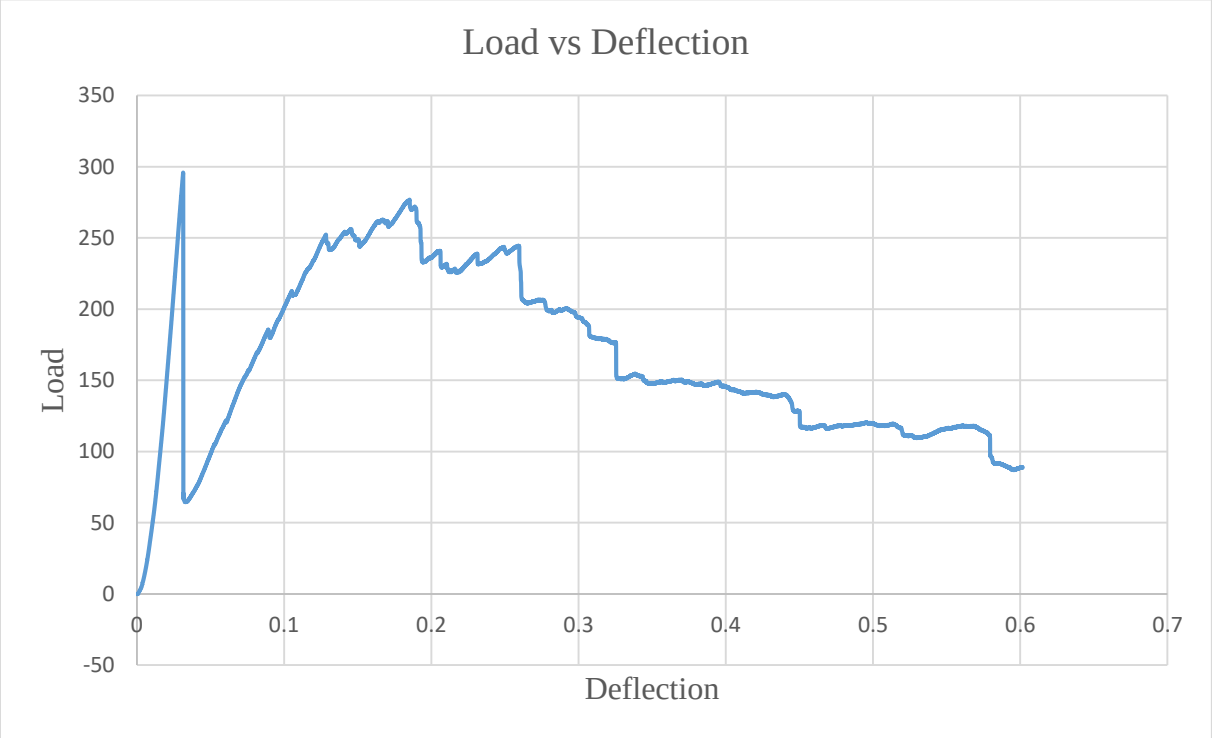

Figure 52 Load-deflection graph for cement-soil specimen reinforced by fiber mesh- Entire diagram

As it can be seen from the load-deflection diagram, there were two phases addressed. The first phase represented the linear elastic region before the crack occurred, while the second phase showed the sample behavior after samples cracked to see the effect of fiber mesh reinforcement on the soil-cement beams. In the first stage, the load was applied and increased linearly with the deflection until the load hit the maximum at 295 lbf and the deflection was 0.0315 inches. After this point, there was a sudden drop of the load from 295 lbfto 67 lbf and the fiber mesh started to work alone. This dramatic drop refers to the weak bonding between the cement-soil material and

the FRP mesh as the mix did not work well together with the FRP mesh. Then, the load was increased again to 261 lbf but it did not exceed the maximum load in the first stage and it decreased once more to the lowest point. Meanwhile, the deflection increased and the load-deflection graph displays a zigzag shape because of the friction between the FRP mesh and the cement-soil material surface. The first phase was the interest point of research as the highest load was achieved in this stage. Hence, the load-deflection and stress-strain diagrams were plotted during the first phase only as follows.

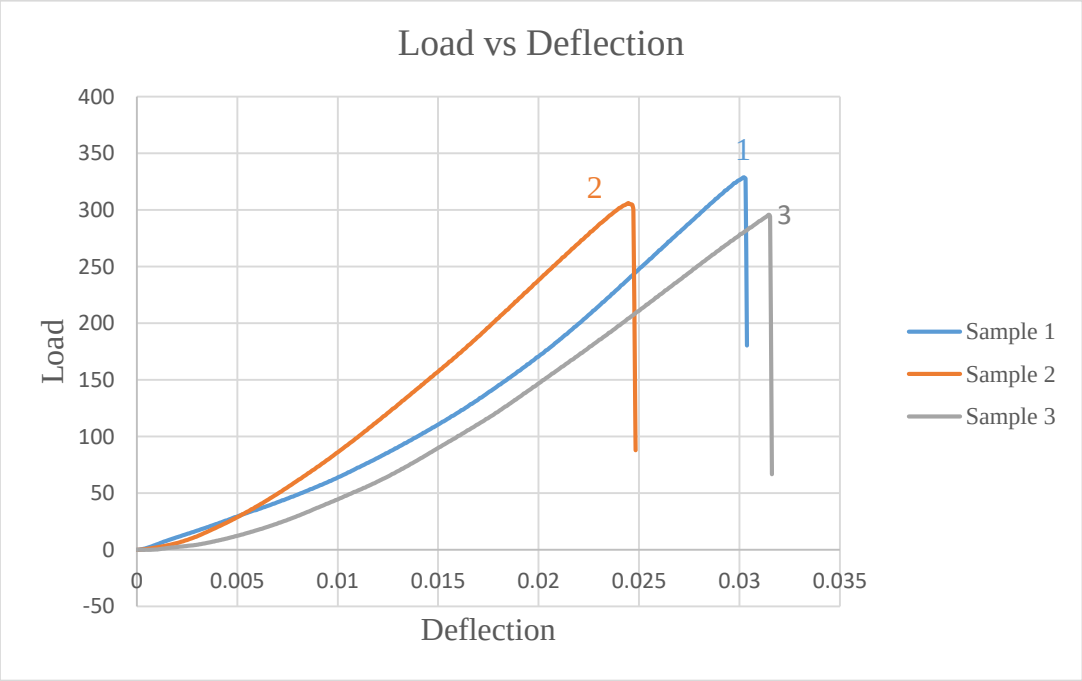

Figure 53 Load-deflection graph for soil until the drop point for soil reinforced by Fiber mesh

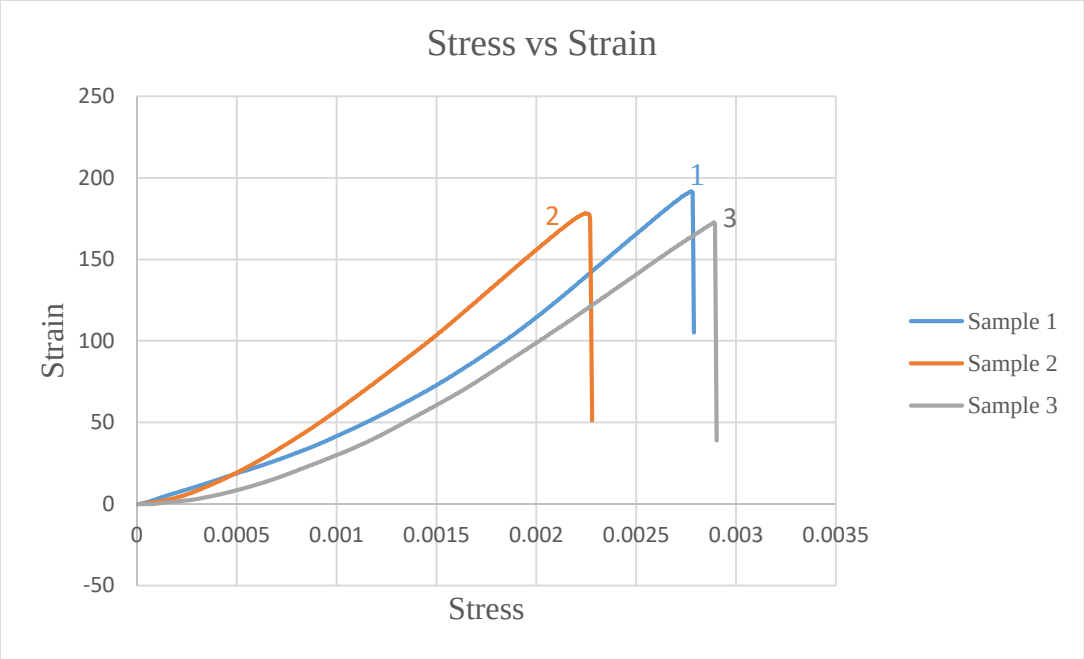

Figure 54 Stress-strain diagram for cement-soil specimen reinforced by fiber mesh

Table 14 Characteristic properties of load-deflection graph

Sample #	1	2	3	Average
Max. Load (lbf)	329	306	296	310
Deflection at Max Load (in)	0.03022	0.02448	0.03148	0.02873
Max. stress (psi)	192	179	173	181
Strain at max Stress	0.002778	0.002248	0.00289	0.00264
Flexural modulus (psi)	66666	77224	60000	67783

In the table above, some of characteristic properties of the three sample were tabulated during the first stage. The three samples had an average maximum load of 310 lfb and average maximum stress of 181 psi. The first sample experienced a deflection of 0.03022 in the maximum load of 329 lbf, while the third sample had a 0.03148 inches at a maximum load of 296.

Furthermore, the flexural modules of the three samples varied between 60000 psi and 77220 psi and the average flexural modulus was nearly 68000 psi.

The pictures below show the flexural crack that formed in the sample:

Figure 55 Pictures of beam reinforced by fiber mesh at failure

5.2.3. Beams made of soil mixed with 12% cement, wrapped, and reinforced with burlap cloth

Another material such as burlap was used to reinforce three beams made of soil mixed with 12% cement. Below loads-deflection and stress-strain diagrams are graphed.

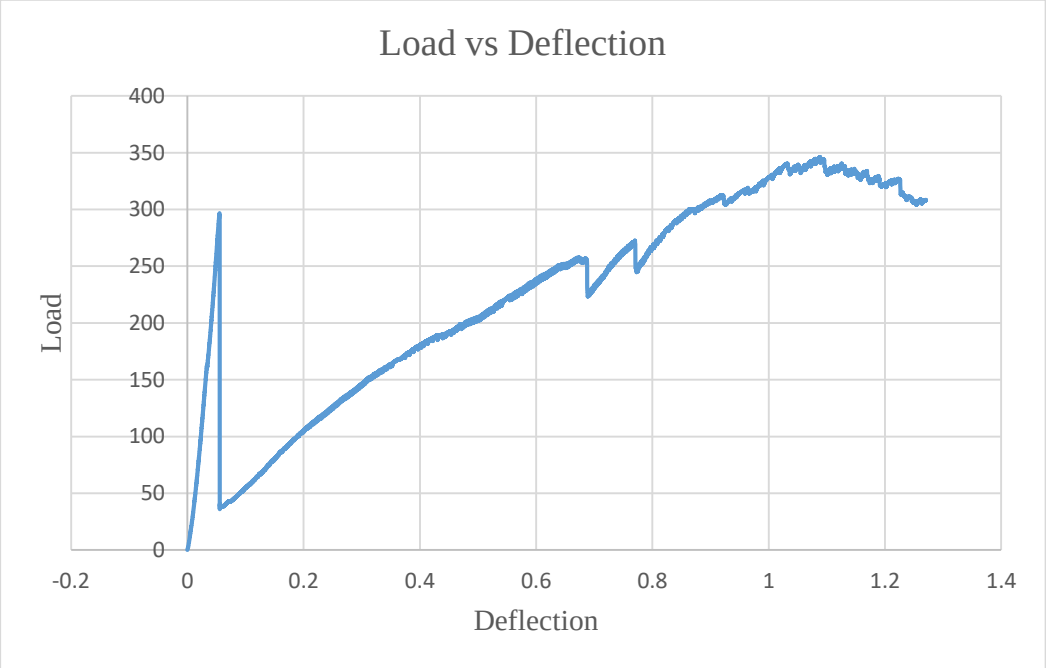

Figure 56 Load-deflection graph for cement-soil specimen reinforced by Burlap cloth- Entire loading

The figure above shows that when the sample was loaded in the first stage, the deflection increased linearly and reached 0.0554 inches when the maximum load was 296 lbf. Then, the beam was cracked and broken so the load fell dramatically below 40 lbf without a deflection increase. The reason of this sudden reduction was that the beam did not work with the burlap as a fully composite body. In fact, the lack of bonding between the beam and the burlap cloth made them work separately. Therefore, during the second stage, the burlap worked alone after this point and the load climbed to 335 lbf before it declined again. Although the load increased to 335 lbf, the beam experienced a large deformation that exceeded 1.2 in. The large deformation was not accepted when considering the serviceability criteria but wrapping the beams by burlap cloths

prevented a catastrophic failure. Throughout the second stage, the load-deflection diagram indicates a zigzag shape because of the friction between the burlap cloth and the beam. Hence, the beams were investigated in the elastic region when the load and the deformation are linearly related.

Figure 57 Loading of specimen wrapped and reinforced by burlap

Figure 58 Failure shape of specimen wrapped and reinforced by burlap

Figure 59 Crack at the maximum load

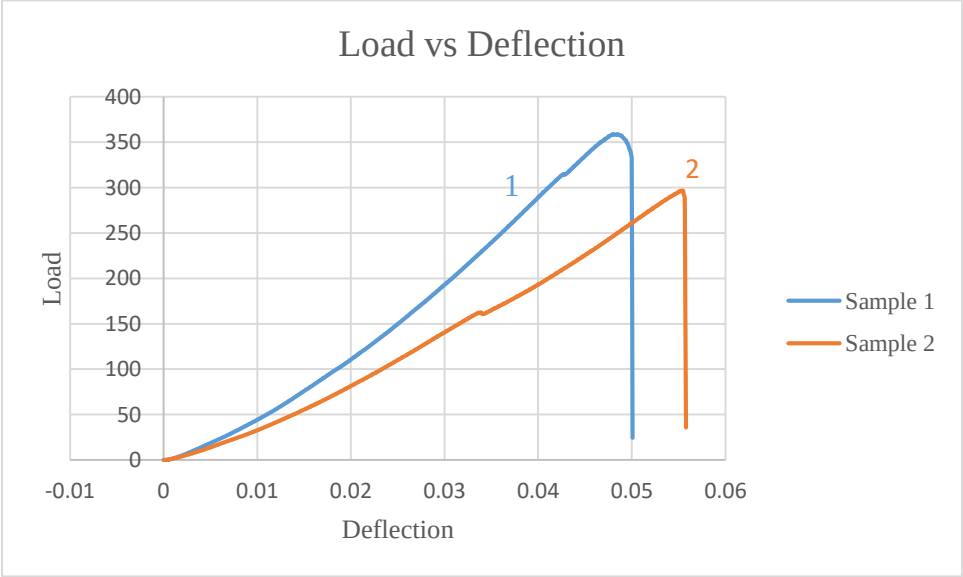

Figure 60 Load-deflection diagram for specimen reinforced by burlap

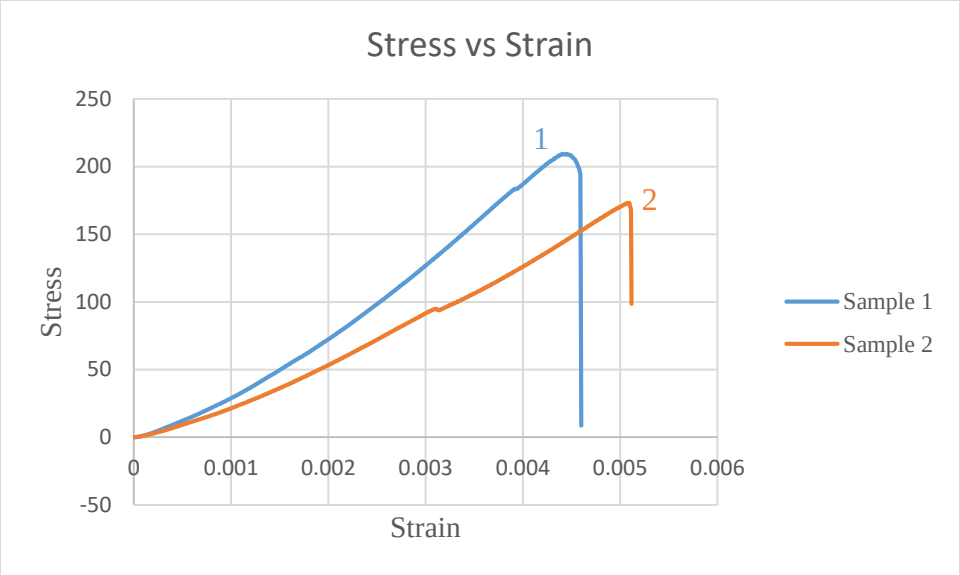

Figure 61 Stress-strain graph for specimen reinforced by burlap

Table 15 Characteristic properties of load-deflection graph for specimen wrapped by burlap

Sample #	1	2	Average
Max. Load (lbf)	360	300	330
Max Deflection at Max Load (in)	0.048	0.056	0.052
Max. stress (psi)	210	173	192
Strain at max Stress	0.00446	0.005094	0.004777
Flexural modulus (psi)	50000	40000	45000

As it is illustrated from the table above, the characteristic properties of two beams are summarized. It shows that the maximum load is between 300 lbf and 360 lbf with corresponding deflections of 0.048 in and 0.056 in respectively. Moreover, the average flexural modulus of both samples is 45000 psi.

5.2.4. Beams made of soil mixed with 12% cement and 2% fiber glass of uncompact volume

In this section, two samples made of soil mixed with 12% cement and 2% glass fiber that were randomly oriented were tested after curing for 7 days instead of 28 days. Load-deflection and stress-strain diagrams are graphed for the purpose of analysis.

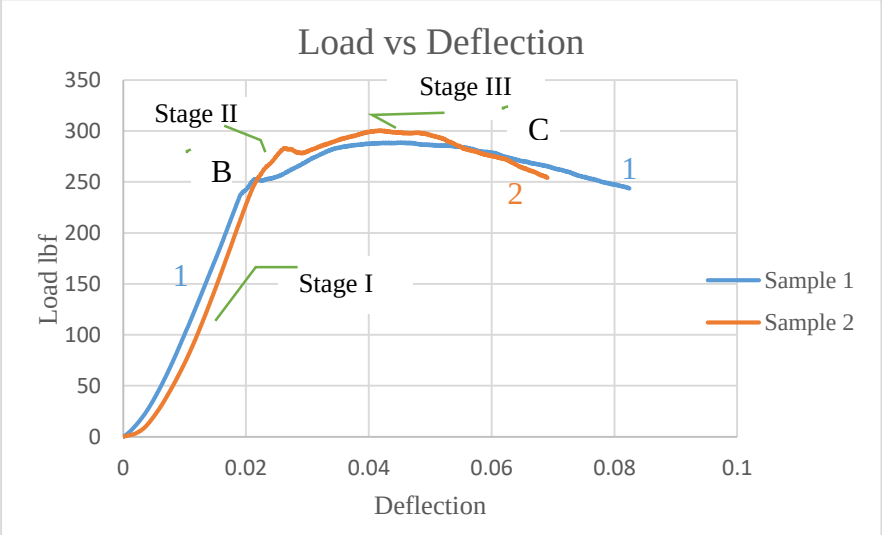

Figure 62 Load-deflection graph of specimen reinforced by glass fiber

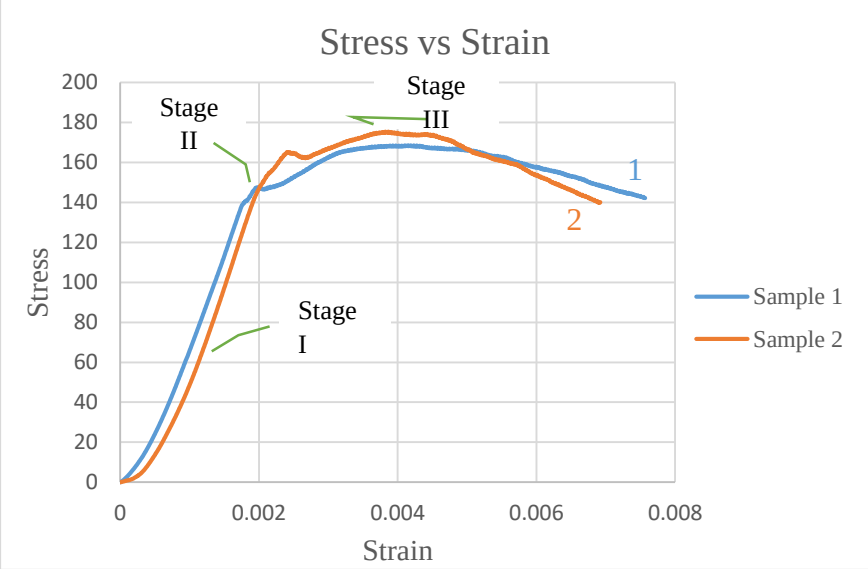

Figure 63 Stress-strain graph of specimen reinforced by glass fiber

As illustrated in the following figures below, the beams went throughout four stages when they were loaded.

The first stage:

Figure 64 The specimen at the first, elastic, stage

At the first stage, the load was small compared with the beams' capacity and the beams experienced an elastic behavior as the load and the stress of the beams were linearly increased with the deflection and the strain respectively up toward the proportional limit; therefore, there was no crack initiation. For example, the load of the first beam increased from zero to 208 lbf and the deflection of the maximum elastic load was 0.019 inches. The elasticity behavior also included the bonding force between the randomly oriented fiber and the mixed materials. Furthermore, at this stage, the neutral axis was located at the center of the beam with a compression stress in the upper part above the neutral axis and the tension stress below it.

The second stage:

Figure 65 The second stage when the crack initiates

At the second stage, the material exhibited a plastic behavior as the load increased beyond the elastic portion and the load-deflection and stress-strain diagrams started to curve toward the yield point. It was observed that there was a small crack that initiated at the bottom of the beam as seen in the figure above, and the fiber created a bridge between both sides of the cracks. Due to the crack initiation, the neutral axis moved up, fiber started extending to pull out, and stress was lost partially at the outermost bottom part of the beam. At this stage, there was a compression zone above the new neutral axis. On the other side, there were two zones below the new neutral axis, an uncrack tension zone and a cracked tension zone.

The third stage:

Figure 66 The third stage

At the third stage, the load increased more with the deflection toward the flexural strength and the material experienced a significant plastic deformation due to the addition of fiber in the mix. As more and larger cracks progressed, the fibers experienced a pull over behavior at the bottom, and the neutral axis moved up more, decreasing the compression zone above it. Throughout the second and the third stages, there was a gradual reduction in the bond between the fibers and the soil-cement material, so there was no sudden drop in the load and the fibers were able to resist more load until the flexural strength.

The final stage:

Figure 67 The final stage when the failure starts

Figure 68 The fiber went out at the bottom of the specimen

After reaching the flexural strength, larger cracks progressed and the beam was fully cracked as the neutral axis went up higher, reducing the compression zone. The lowest fibers of

the beam deformed and went out of the mix and they were not able to resist any load. Next, the load decreased gradually without any sudden drop until a complete failure occurred.

Furthermore, the flexural character's properties of the two beams are tabulate below:

Table 16 Characteristic properties of specimen reinforced by glass fiber

Sample #	1	2	Average
Max. Load (lbf)	290	300	295
Deflection at Max Load (in)	0.0419	0.04163	0.04177
Yielding stress (psi)	168	174	171
Max. stress (psi)	169	176	173
Strain at max tress	0.0039	0.004	0.00395
Flexural modulus (psi)	88447	89100	88774

Both beams exhibited a close match of behavior and values. They have an average maximum load of 295 when the deflection was in range between 0.04565 inches and 0.04492 inches. The flexural stresses they experienced were 169 psi and 176 psi for the first and the second beam respectively. Furthermore, there was a clear yield point as the beams experienced a large deformation with a small increase of the load. Hence, there was a plasticity exhibited after the yield point and the beams were able to absorb large energy. Using 0.2% set, the average yield stress for the samples was 171 psi. Final point to mention, the flexural modulus of the samples was around 89000 psi. The first beam had a flexural modulus of 88450 psi, while the second beam had a slight higher number, standing at 89100 psi.

5.2.5. Flexural results comparisons

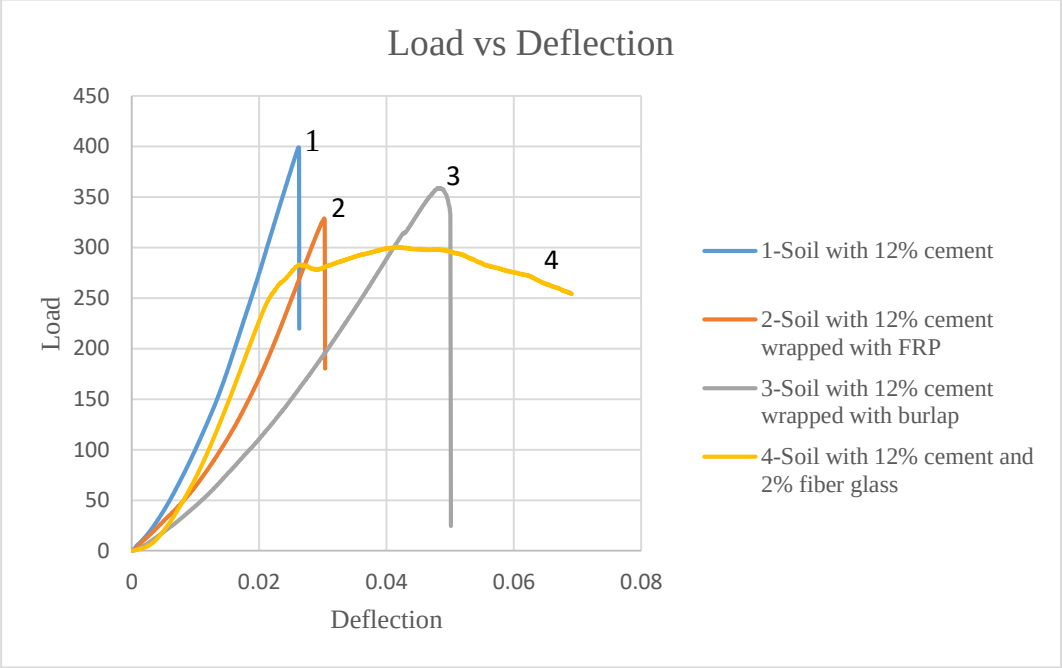

Table 17 Load-deflection graphs of the four types of beams

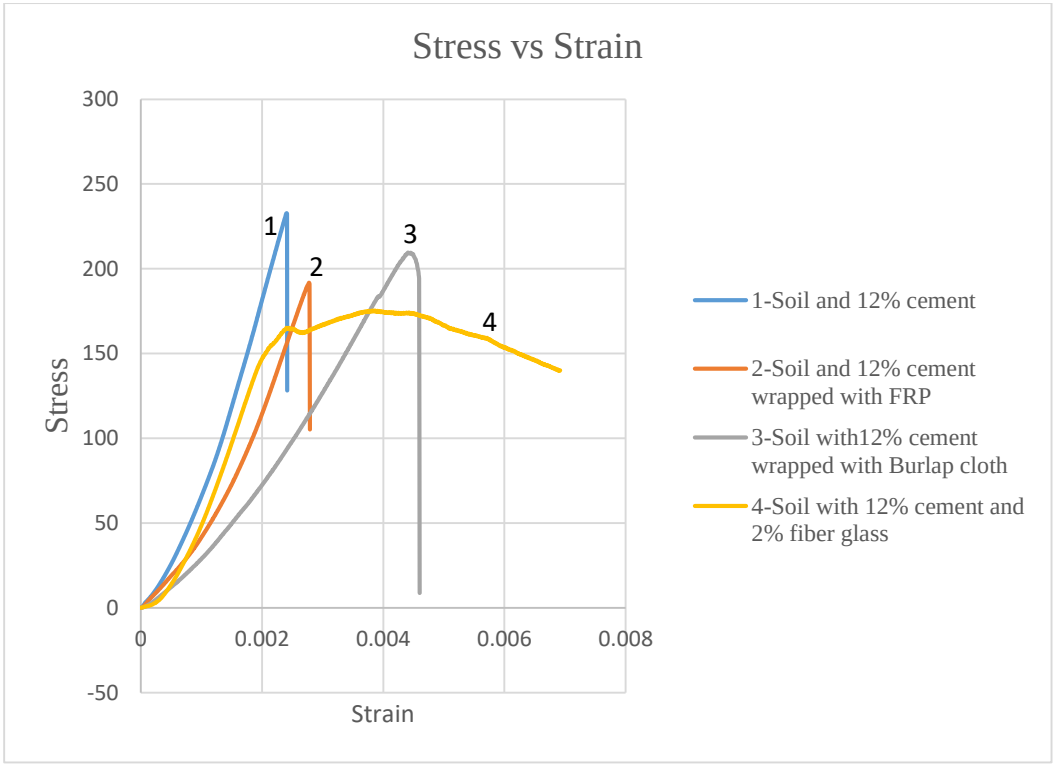

Table 18 stress-strain graphs of the four types of beams

Table 19 summery of characteristic properties of the four beam at particular curing age

Sample made of soil and	Cement	Cement and FRP	Cement and Burlap	Cement and Fiber Glass
Curing (days)	28	28	28	7
Max. Load (lbf)	360	310	330	295
Max Deflection at Max Load (in)	0.0266	0.02873	0.052	0.0417
Yielding stress (psi)	-	-	-	171
Max. stress (psi)	205	181	192	173
Strain at max Stress	0.00243	0.00264	0.004777	0.00395
Flexural modulus (psi)	80000	67783	45000	88774

The flexural properties of different reinforced beams are presented in the figures 15and16 and the table 17 above to identify the effect of each type of reinforcement on the flexural properties of beams subjected to three-point loading test. These beams were investigated individually in the preceding paragraphs and they were mainly made of soil-cement material reinforced by FRP mesh, burlap cloth, or chopped fiber glass. All of beams were cured for 28 days except the beam reinforced by chopped fiber glass which was tested after 7 days of curing.

The cement-soil beam was loaded after 28 days of curing to a maximum load of 360 lbf, while the beams reinforced by FRP or burlap were not able to resist this load and they fractured at 310 lbf and 330 lbf respectively. The beam that was reinforced by glass fiber resisted a maximum load of 295 lbf after curing for seven days. Therefore, it was predicted that after 28 days, this type of beam would achieve a flexural strength that is much larger than the all other beams' strength. Furthermore, it was reported that adding glass fiber to the cement-soil material improved the

flexural modulus. In fact, the flexural modulus of the beams reinforced by fiber glass peaked at 89000 psi and it was higher than 80000 psi, which was the flexural modulus of beams made of soil and cement. This modulus reduced nearly 50% to 45000 psi when the cement-soil beam was wrapped by burlap cloth. Beams wrapped by FRP mesh had a flexural modulus of 67000 psi which is less than the flexural modulus of beams mixed with or without fiber glass.

An important point to emphasize is that only the beam reinforced by fiber glass exhibited a ductility after the flexural peak and it was able to absorb a large amount of energy without failure. As it is illustrated from the stress-strain figure, after the stress reached the lower yield point at 155 psi, the stress experienced a hardening increasing toward the flexural strength at 172 psi with a large increase of the strain. After the stress peak point, the beam continued to deform, absorbing larger amount of energy without any increase of the stress. This can be seen by the area under the stress-strain diagram. Next, the stress decrease gradually to the failure point. On the other hand, no plastic deformation was observed in the other samples that were not reinforced by fiber glass. There was a sudden failure when the stress of the beam made of soil and 12% cement increased to 205 psi. Moreover, the beams reinforced with FRP mesh or burlap cloth also underwent a sudden drop which exceeded 90% of the maximum stress before it rose.

These unsatisfying results were due to the weak bond between the FRP mesh or the burlap cloth and the cement-soil material. Hence, instead of increasing the strength, the flexural strength of wrapped beams was reduced when compared with the flexural strength of the unreinforced beams made of soil mixed with 12% cement.

Consequently, it was concluded that adding glass fibers to the cement-soil mix enhanced the flexural behavior by increasing the flexural strength and the ability to absorb higher energy. When more fiber crosses the cracks, higher flexural strength is achieved. Opposite to the burlap and FRP

mesh, the glass fiber provides a strong bonding with the soil mix. Therefore, bond plays an important role in improving the flexural behavior. However, bond is influenced by various factors such as the orientation and the shape of fiber. In the case of the beams tested in this research, it will be more effective when the fibers are oriented in a perpendicular direction to the cracks. Then the fibers cross the cracks and increase the strength.

5.3.Heat loss results

As it was mentioned in the heat loss measurement, temperature was measured at interval times of 10 minutes. The temperature was tabulate in the following table:

Table 20 Reading of sample temperature

TIME [m]	Inside [F]	Outside [F]
0	473	290
5	408.2	266
15	332.6	223
25	262.4	189
35	208.22	158
45	171.5	137
55	145.4	120
65	127.4	108
75	113.54	98
85	103.46	92
95	95.9	91
105	90.14	86
115	85.64	80
140	82.4	77
150	79.7	76
160	77.9	74.5
170	76.1	73.5
180	74.3	72.5
190	72.5	71.5
200	70.7	70
205	70.0	70

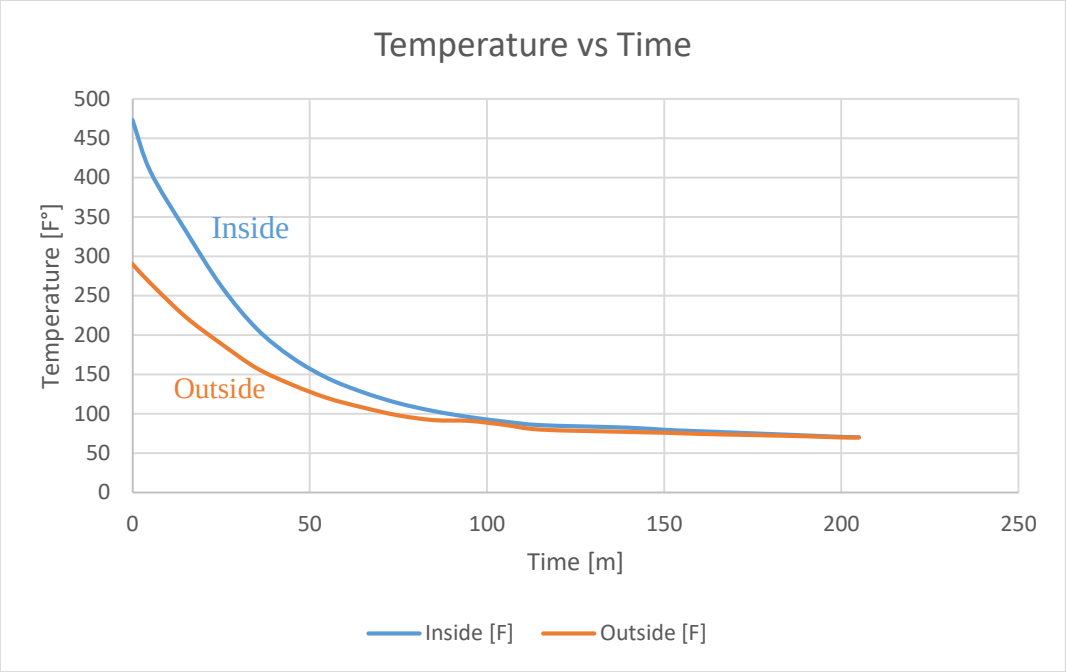

Figure 69 heat loss vs time

The rammed earth construction system has become more popular because of the material components properties. Not only, they have inexpensive, but also they have a low thermal conductivity.

As mentioned previously by Milani and Labaki (2012), the thermal conductivity for 100% soil stabilized with 10% cement was 0.8W/mk and it dropped to 0.65 W/mK when 7.5% rice hush ash was added to the cement-soil mix.

The thermal conductivity of the soil used in this study was calculated using equation proposed by Johansen:

$$K = \frac{0.135\,\gamma_d + 64.7}{2700 - 0.94\,\gamma_d} \pm 20\%$$ Johansen 1975

$\boldsymbol{\gamma}_d$: The dry density of the soil (kg/m^3) = 1830 kg/ m^3 (in this study)

The thermal conductivity K = $\frac{0.135\ (1830)+64.7}{2700-0.94\ (1830)} \pm 20\%$ = 0.318177 ± 20% W/mK

It is can be concluded that the thermal conductivity of soil is low.

6. Conclusions

There is growing interest in using natural materials with low carbon and more sustainability in building construction as it has a good performance in heat resistance, durability, and structural capability. Adding different types of materials was investigated to find the effect of this material on the soil properties. In this research, different ratios of fly ash, and/or cement were added to the soil to improve the compressive strength. However, recycled fiber materials were used to wrap and reinforce the cement-soil specimens in order to enhance the flexural strength and control the cracks and the mode of failure.

It can be concluded that adding fly ash to soil sample results in elastic modulus reduction. Moreover, it was observed that while a sample made of soil has an ultimate compressive strength of 171 psi, it increased to 1450 psi when 12% cement is added, therefore, adding cement to soil has significant effect on the soil strength, and it causes a remarkable growth in the strength. On the other side, it is concluded that adding fly ash only to soil does not affect the strength. It remains similar to specimens made of soil only. Furthermore, the ultimate strength of soil mixed with 6% fly ash and 6% cement stands in the middle place between the soil samples and soil-stabilized with 12% cement with an ultimate strength value of 700 psi.

Comparing to concrete specimen, the concrete compressive strength is 5500 psi and it is three times larger than compressive strength of cement-soil samples that hit 1450 psi. moreover, the Young's modulus of concrete is 3645000 psi which is 50 times larger than the elastic modulus of soil samples stabilized with 12% cement.

Furthermore, three-point loading test was conducted to determine the flexural properties of four types of specimens. It was concluded that soil-cement specimens resisted an average maximum load of 360 lbf after curing for 28 days, while the beams reinforced by FRP or burlap

cloth were not able to resist this load and they fractured at 310 lbf and 330 lbf respectively at the same age of curing. Wrapping beams by burlap or fiber mesh will prevent a catastrophic failure. However, the beam that was reinforced by glass fiber resisted a maximum load of 295 lbf after curing for seven days only. Therefore, it was predicted that after 28 days, this type of beam would achieve a flexural strength that is much larger than the all other beams' strength. Furthermore, it was reported that adding glass fiber to the cement-soil material improved the flexural modulus. In fact, the flexural modulus of the beams reinforced by fiber glass peaked at 89000 psi and it was higher than 80000 psi, which was the flexural modulus of beams made of soil and cement. This modulus reduced nearly 50% to 45000 psi when the cement-soil beam was wrapped by burlap cloth and to 67000 psi when the specimen wrapped by fiber mesh. An important point to emphasize is that only the beam reinforced by fiber glass exhibited a plastic behavior after the flexural peak and it was able to absorb a large amount of energy without failure. While the other types of beams experienced a sudden drop and failure. Furthermore, opposite to the burlap and FRP mesh, the glass fiber provides a strong bonding with the soil mix so adding glass fibers to the cement-soil mix enhanced the flexural behavior by increasing the flexural strength and the ability to absorb higher energy.

References

1. ASTM. (2007). “Standard test methods for Flexural Performance of Fiber-Reinforced Concrete (Using Beam with Third-Point Loading).” C 1609/C 1609M – 06.
2. Burroughs, S. (2008). “Soil Property Criteria for Rammed Earth Stabilization.” Journal of Materials in Civil Engineering, J. Mater. Civ. Eng. 2008.20:264-273. (2008) 20:3(264).
3. Ciancio, D., Robinson, S. (2011) “Use of the Strut-and-Tie Model in the Analysis of Reinforced Cement-Stabilized Rammed Earth Lintels” Journal of Material in Civil Engineering, Vol. 23, No. 5, May 1, 2011. 587–596
4. Corbin, A., Augrade, C. (2014) “Fracture Energy of Stabilized Rammed Earth.” Procedia Material Science 3 (2014) 1675-1680
5. Easton, D. (1982). The rammed earth experience, 1st Ed., Blue MountainPress, Wilseyville, CA.
6. Jayasinghe, C., Kamaladasa, N., (2007) “Compressive strength characteristics of cement stabilized rammed earth walls” Construction and Building Materials, 21 (2007) 1971–1976
7. Cong Ma, C., Chen, L., Chen, B., (2016) “Experimental Study of Effect of Fly Ash on Self-Compacting Rammed Earth Construction Stabilized with Cement-Based Composites.” J. Mater. Civ. Eng., 2016, 28(7): 04016022
8. Maniatidis, V., Walker, P., “Structural Capacity of Rammed Earth in Compression.” J. Mater. Civ. Eng., Vol. 20, No. 3, March 1, 2008. 230–238
9. Milani, A., Labaki, L., (2012) “Physical, Mechanical, and Thermal Performance of Cement-Stabilized Rammed Earth–Rice Husk Ash Walls.” J. Mater. Civ. Eng., Vol. 24, No. 6, June 1, 2012. 775–782

10. Prasanna Kumar P, Venkatarama Reddy BV, (2011) “Cement stabilised rammed earth. Part B: compressive strength and stress–strain characteristics” Materials and Structures (2011) 44:695–707, DOI 10.1617/s11527-010-9659-8
11. Prasanna Kumar P, Venkatarama Reddy BV, (2011) “Cement stabilised rammed earth. Part A: compaction characteristics and physical properties of compacted cement stabilised soils” Materials and Structures (2011) 44:681–693, DOI 10.1617/s11527-010-9658-9
12. Tripura, D., Singh, K.D., (2015) “Characteristic Properties of Cement-Stabilized Rammed Earth Blocks” J. Mater. Civ. Eng., 2015.27. 04014214-1
13. Tang, C.S., Wang, D.y., Cui, Y.J., Shi, B., Li, J., (2016) “Tensile Strength of Fiber-Reinforced Soil” J. Mater. Civ. Eng., 2016, 28(7): 04016031